

SUPPORTING INFORMATION

Molecular Recognition and Proteoglycan Mimic Arrangement: Modulating Cisplatin Toxicity

Saurabh Anand, Sandhya Mardhekar, Preeti Ravindra Bhoge, Sandeep Kumar Mishra,
Raghavendra Kikkeri.

Indian Institute of Science Education and Research, Dr. Homi Bhabha Road, Pashan, Pune-
411008, Maharashtra, India

Email. rkikkeri@iiserpune.ac.in

Table of contents

1. General information
2. NMR Studies of **G12** and **I12** ligands and complex formation with cisplatin
 - 2a. Correlation Time-Induced Relaxation Studies
 - 2b. Diffusion Ordered Spectroscopy (DOSY)
 - 2c. Detection of conformational changes by ^1H and ^{13}C NMR after the addition of cisplatin
3. Rate of formation of the complex
4. Synthesis of fluorescent probe
5. Synthesis of cholesterol linker
6. Synthesis of neoproteoglycan (**P-I12**)
7. Cell surface engineering studies
8. Co-localization studies
9. Pathway Study
10. MTT assay
11. ICP-MS Analysis
12. References
13. ^1H -NMR, ^{13}C and DEPT-135 NMR
14. HPLC profile of **P-I12**.

1. General Information

All chemicals were reagent grade and used without further purification unless otherwise noted. Reactions were carried out in anhydrous solvents under a nitrogen atmosphere. Reaction progress was monitored by analytical thin-layer chromatography (TLC) on Merck silica gel 60 F₂₅₄. Spots on TLC plate were visualized under UV light or by dipping the TLC plate in CAM/ninhydrin solution followed by heating. Column chromatography was carried out using Fluka kieselgel 60 (230-400 mesh). ¹H and ¹³C NMR spectra of compounds were measured with Bruker 400 MHz, Bruker 600 MHz and Jeol 400 MHz using residual solvents as an internal reference (CDCl₃ δH 7.26 ppm, δC 77.3 ppm, CD₃OD δH 3.31 ppm, δC 49.0 ppm, and D₂O δH 4.79 ppm). The chemical shifts (δ) are reported in ppm and coupling constants (J) in Hz. UV-visible measurements were performed with Evolution 300 UV-visible spectrophotometer (Thermo Fisher Scientific, USA). Fluorescence spectra were measured with FluoroMax-4 spectrofluorometer (Horiba Scientific, U.S.A.). For colocalization studies EEA1 antibody (MA5-31575, early endosomal marker), LAMP2 antibody (MA1-165, late endosomal marker), Donkey anti Rat IgG (H+L) highly cross absorbed secondary antibody Alexa fluor 488 (A48269), LysoTracker green (L7526) purchased from eBioscience™. All microscopy images were captured using Leica SP8 confocal microscope and processed using Image J software. Synthesis of **G12** and **I12** is already reported in our previous publications.¹

2. NMR Studies of **G12** and **I12** ligands and complex formation with Cisplatin

Uronic acid compounds (**G12** and **I12**) (1 mM) were mixed with cisplatin (1 mM) in D₂O solvent and used as such for all NMR studies.

2a. Correlation Time-Induced Relaxation Studies

According to the Bloembergen-Purcell-Pound (BPP) theory proposed by Nicolaas Bloembergen, Edward Mills Purcell, and Robert Pound, the relaxation times of a pure substance (in NMR) are approximately related to the molecular correlation time (τ_c). The correlation time (τ_c) is the time a molecule takes to undergo rotation by one radian (57.296°), and it depends on the size of the molecule while keeping all other physical parameters constant. The qualitative representation of T₁ and T₂ dependency on correlation time is given in **Fig. S1**. Where T₁ is the longitudinal or spin-lattice relaxation time constant, and T₂ is the transverse or spin-spin relaxation time constant. When a small molecule interacts with

another larger molecule or with proteins, its relaxation time changes substantially and can be used as evidence for intermolecular interactions. There is no significant effect of intramolecular interaction on the relaxation in NMR as the size of the molecule doesn't change in such a situation.

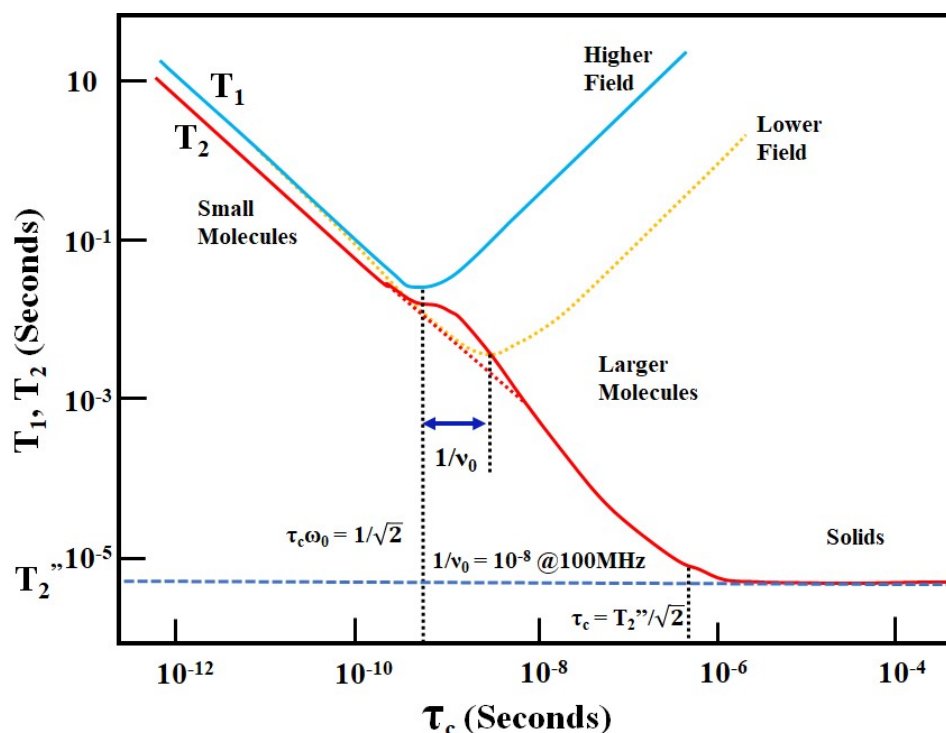


Figure S1. The behaviour of relaxation times as a function of correlation time (τ_c) for spin $\frac{1}{2}$ nuclei relaxing by the Dipole-Dipole mechanism. Adapted with permission from ref 2. and used after modification.

The best way of relaxation study for testing the intermolecular interaction is monitoring the change in the molecule of smaller size as the changes in small molecules reflect substantially compared to the large molecule. This is because the sum of the correlation time (τ_c) is observed after interaction and the net change in the size of a larger molecules is less for the larger molecules as size of ligand or small molecules is nominal to the size ratio. Unfortunately, in our system, the cisplatin has no detectable protons or carbons; hence the resonances of glucose derivatives **G12** and **I12** are observed.

In addition to size, the relaxation is also residue-specific; hence the substantial change in T_1 could be observed for the binding sites of glucose derivatives. The relaxation rate for ^1H at C4 was observed faster in **G12** with cisplatin due to the restriction in motion by hindrance at that position. On the other hand, the rate of relaxation for ^1H at C2 is observed faster in **I12** after interaction with the cisplatin. The above observations indicate that the binding site in

G12 is at C4, and C2 in the **I12**. In other words, the sulphate group at C4 in **G12** and C2 in **I12** is the interaction site for cisplatin in these molecules. The ^1H NMR spectra of T1 studies on **G12** and **I12**, with and without the addition of cisplatin are compared and given in Figure S2.

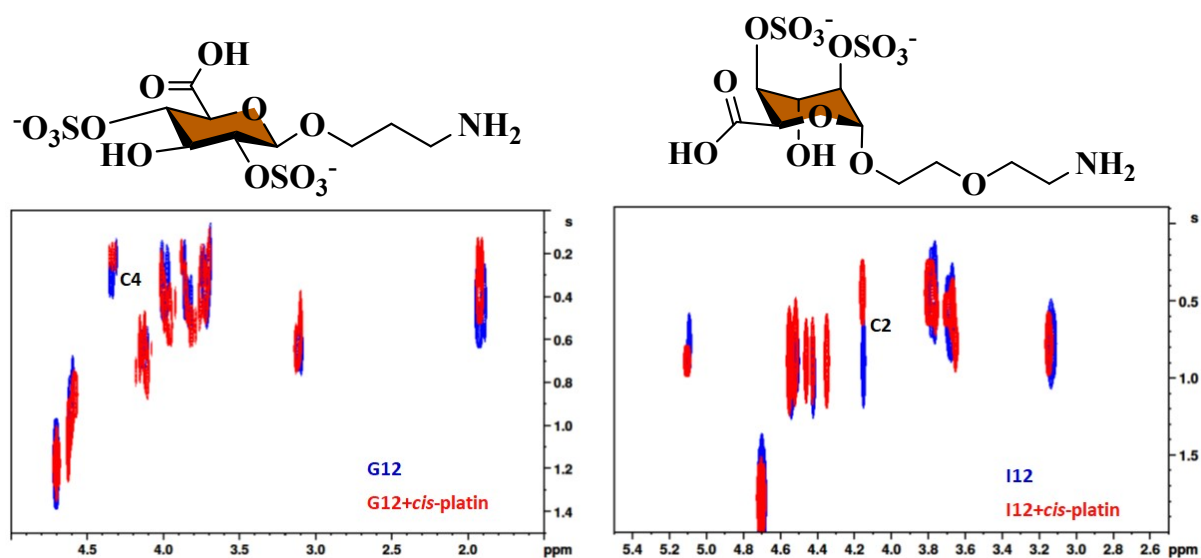


Figure S2: The stacked 400 MHz ^1H NMR spectra for T1 studies acquired using an inversion recovery pulse sequence. The particular colour for identification purposes highlights the colour-coded contours and the compounds.

2b. Diffusion Ordered Spectroscopy (DOSY)

The DOSY in NMR has appeared as an effective tool in studying non-covalent intermolecular interactions between two or more molecules in solution. The diffusion coefficient is inversely proportional to the molecular hydrodynamic radius (molecular size). Since the diffusion coefficient depends on the size and intermolecular interactions, it results in the addition in size and reduction in diffusion rates. The NMR spectroscopy can be utilized in translational diffusion measurement using a pulsed-field gradient (PFG). The PFG produces a variation in the linear magnetic field across the NMR sample, which leads to the variation in the precession frequencies for a particular signal as it depends on the effective magnetic field. The signal evolution in the presence of PFG is refocused by another PFG of the same duration and strength after the magnetization inversion by 180° radio frequency pulse. This refocusing is only effective in the absence of diffusion in the sample, and the translational diffusion results in a magnetization decay as δ .

$$I = I_0 e^{-D(\gamma\delta G)^2 (\Delta-\delta/3)}$$

Where I represent the intensity observed after the refocusing gradient, I_0 is the intensity without gradient, D stands for the diffusion coefficient, γ is the gyromagnetic ratio, δ is the gradient duration of strength G , and Δ is the delay between both the gradients.

With the knowledge of diffusion constants (D), the formula weights (FW) of a molecule or system can be derived from the relationship-

$$\log D \propto \log \text{FW}$$

The estimated formula weight effectively approximates the number of interacting molecules and their ratio. The spin-echo diffusion method with PFG³ has been broadly applied in investigating intermolecular HB, ion-pairing, aggregation, π - π stacking in supramolecular chemistry.⁴ and the transition metal catalysts.⁵ The DOSY has been used in determining the formula weights of polymers and the structures of organometallic complexes in solution.⁶ The DOSY technique is also useful in examining the absence or presence of intermolecular interactions or molecular aggregation.

The free molecules have a particular diffusion rate, and it is observed slower if they interact with other molecules as the hydrodynamic radius increases. This technique has proven effective in examining the protein-ligand interaction. where the diffusion coefficient of a small ligand changes drastically if bound to a huge protein molecule. Due to the faster decay in the diffusion filter, small free molecules with fast diffusion that are free can be removed from the spectrum, and the molecules that bind to a large biomolecule remain in the spectrum because of their significantly slower diffusion.

Similar to the relaxations studies, the intermolecular interactions are monitored as a change in the molecular size (hydrodynamic radius) after interaction between two or more molecules. There is a substantial observable change for the smaller molecules compared to the large molecule. This is because the sum of the hydrodynamic ratio is observed after the interaction, which changes nominal for the larger molecules as the size of the ligand or small molecules is comparatively less. In our system, the smaller molecule cisplatin does not have any detectable protons or carbons; hence the change in the rate of diffusion after the addition of cisplatin is studied for the resonances of glucose derivatives **G12** and **I12**.

For diffusion studies, the pseudo-2D ¹H DOSY experiments with and without the addition of cisplatin were carried out for both the studied glucose derivatives **G12** and **I12**. All the physical parameters (before and after adding cisplatin) were kept identical for comparison purposes. The obtained DOSY spectra on **G12** molecule in both conditions are qualitatively compared in Figure S3. On careful inspection, it was observed that a slower rate of diffusion

is observed after adding cisplatin to **G12**, which indicates the increase in Stokes or hydrodynamic radius, hence the molecular size. This increase in the molecular size of the glucose derivative **G12** is attributed to the association of cisplatin with it.

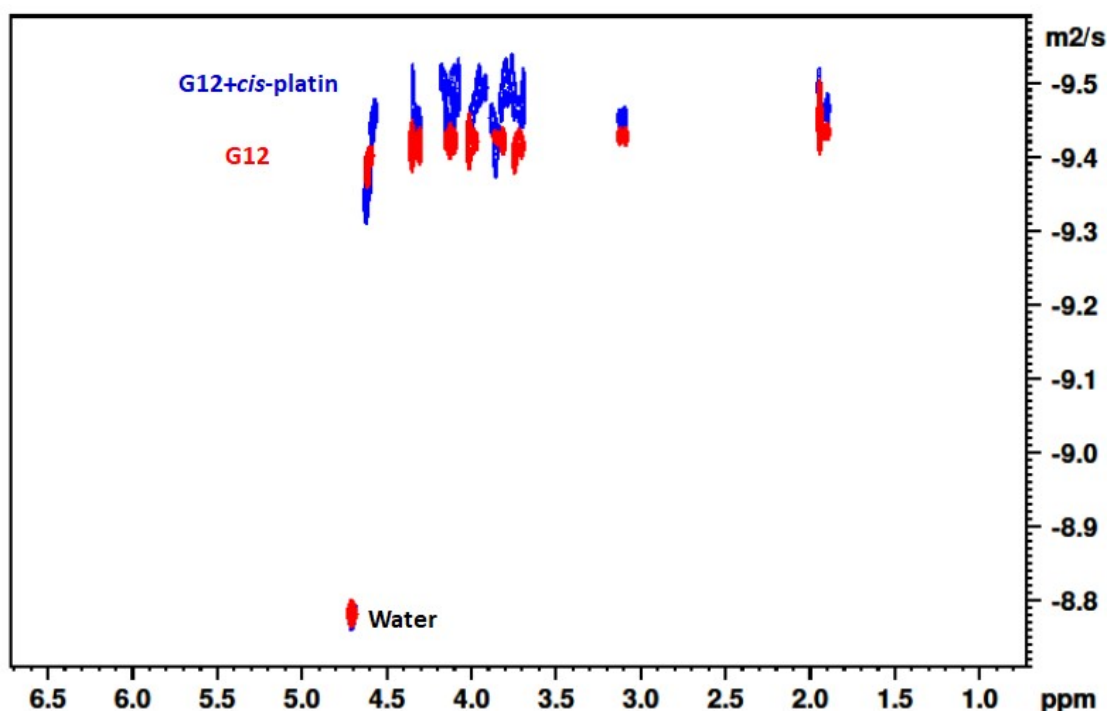


Figure S3: The comparison of diffusion rates for the G12 (red) and G12+cisplatin (blue). Water resonance is used as the reference and calibrated at the same diffusion rate (with and without cisplatin).

The diffusion data of **G12**, with and without cisplatin, was also analysed quantitatively and the obtained results were compared with the diffusion rates of the residual protons of solvent D₂O. The diffusion rate (*D*) for water in **G12** was observed $1.62 \times 10^{-9} \text{ m}^2\text{s}^{-1}$, and it was $37.1 \times 10^{-9} \text{ m}^2\text{s}^{-1}$ for the **G12**. Interestingly after the addition of cisplatin, the rate of diffusion for water remained the same, but the diffusion of **G12** resonance was observed slower, i.e. $31.8 \times 10^{-9} \text{ m}^2\text{s}^{-1}$, which gives a piece of clear evidence for the interaction between **G12** and cisplatin. The plots of the diffusion rates of the randomly selected resonances of **G12** (with and without cisplatin) and water of both the samples are compared in the Figure S4.

Using *D* value, the Stokes radius (*R_s*) for **G12** was calculated 0.66 nm and 0.77 nm for the G12+cisplatin. The increase in *R_s* is evident in the increased hydrodynamic radius of **G12** due to the interaction with cisplatin.

^1H DOSY analysis of G12 and G12+*cis*-Platin

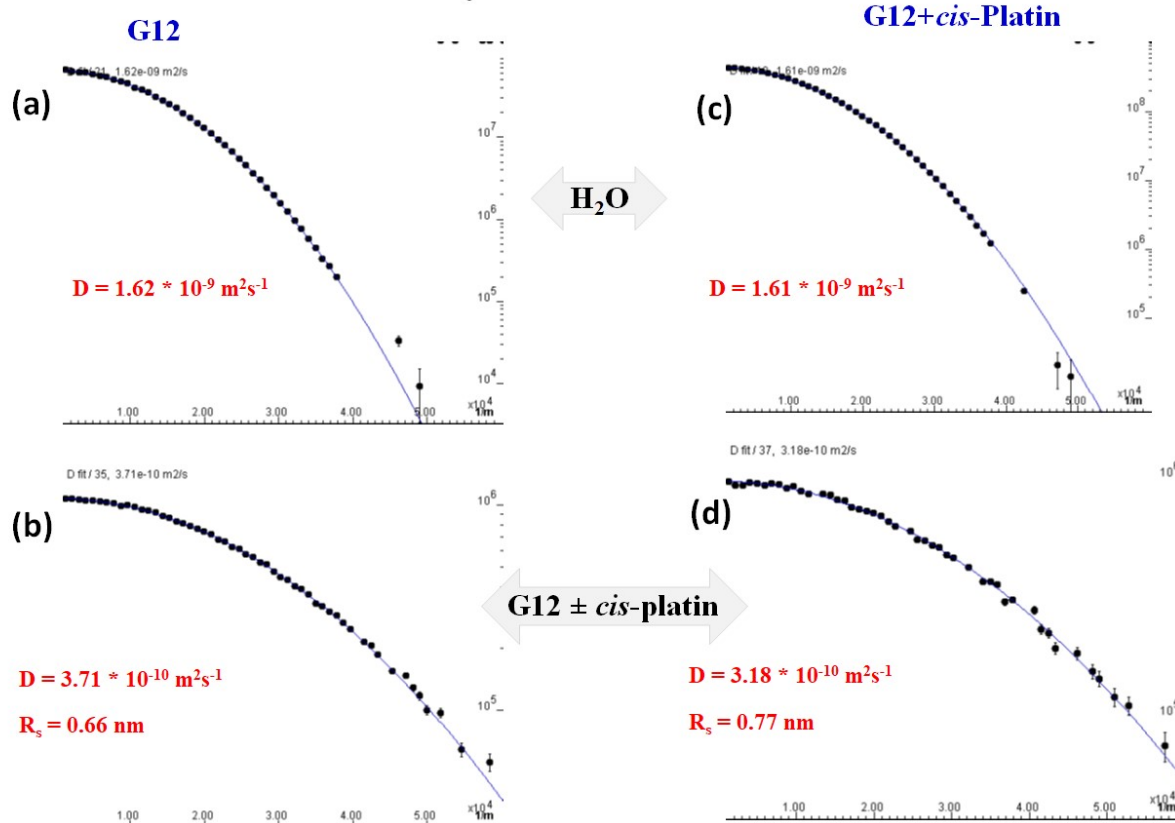


Figure S4. The quantitative analysis of diffusion data of G12 before and after the addition of *cis*platin, the plot of rate of diffusion for (a) residual water in G12 (b) a randomly selected resonance of G12 (c) residual water after the addition of *cis*platin and (d) G12+*cis*platin. The data was plotted using Bruker Dynamics Center 2.8.0.1 software in automation mode.

The obtained DOSY spectra of the I12 molecule with and without *cis*platin are qualitatively compared in the Figure S5. On careful comparison, the slower rate of diffusion is observed after adding *cis*platin to I12, which indicates the increase in Stokes or hydrodynamic radius, hence the molecular size. This increase in the molecular size of the glucose derivative I12 is attributed to the association of *cis*platin with it.

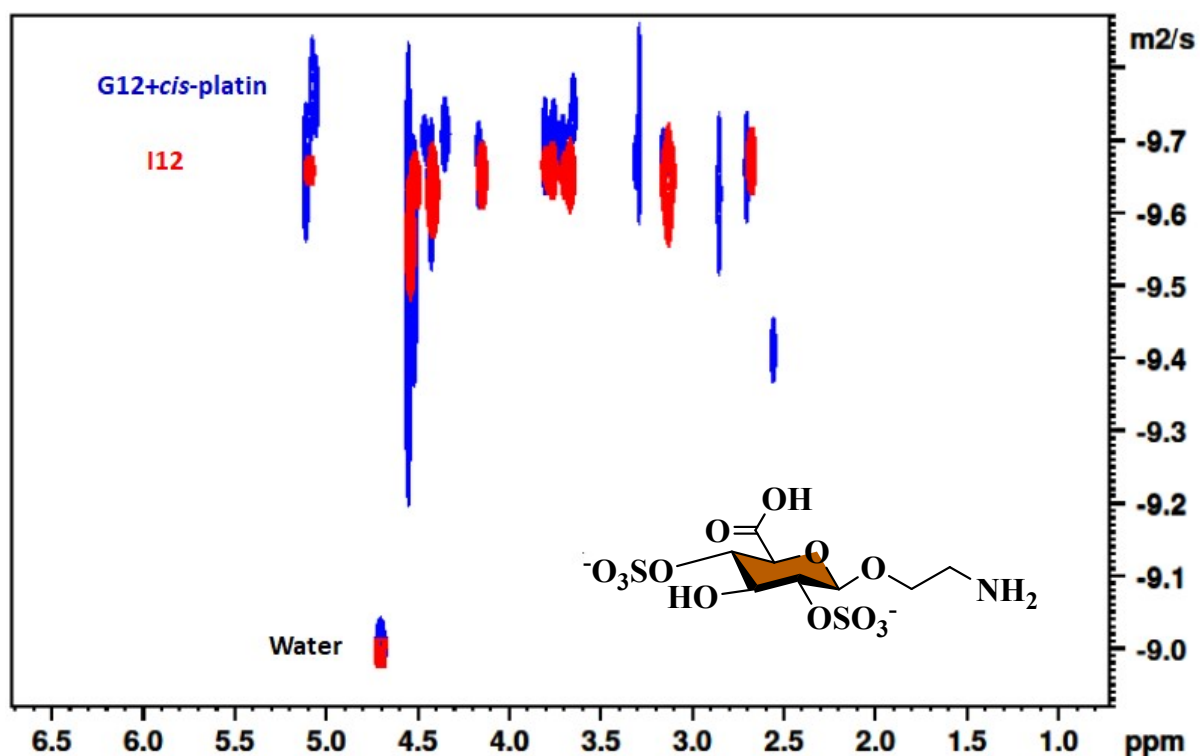


Figure S5: The comparison of diffusion rates for the I12 (red) and I12+cisplatin (blue). Water resonance is used as the reference and calibrated at the same diffusion rate.

The Diffusion data for **I12**, with and without cisplatin, was also analysed quantitatively, and the obtained results were compared with the diffusion rates of the residual protons of solvent D_2O in both conditions. The diffusion rate (D) for water in **I12** was observed $9.73 \cdot 10^{-10} \text{ m}^2 \text{ s}^{-1}$, and it was $2.23 \cdot 10^{-10} \text{ m}^2 \text{ s}^{-1}$ for the **I12**. Interestingly after the addition of cisplatin, the rate of diffusion for water remained the same, but it was observed slower i.e. $2.04 \cdot 10^{-10} \text{ m}^2 \text{ s}^{-1}$ which gives a shred of clear evidence for the interaction between **I12** and cisplatin. The plots of the diffusion rates of the randomly selected resonances of **I12** (with and without cisplatin) and water of both the samples are compared in the Figure S6.

Using the value of D the Stocks radius (R_s) for **I12** was calculated 1.1 nm, and it was 1.12 nm for the I12+cisplatin. The increase in the R_s is also evident in the increased of **I12** due to the interaction with cisplatin.

¹H DOSY analysis of I12 and I12+cis-Platin

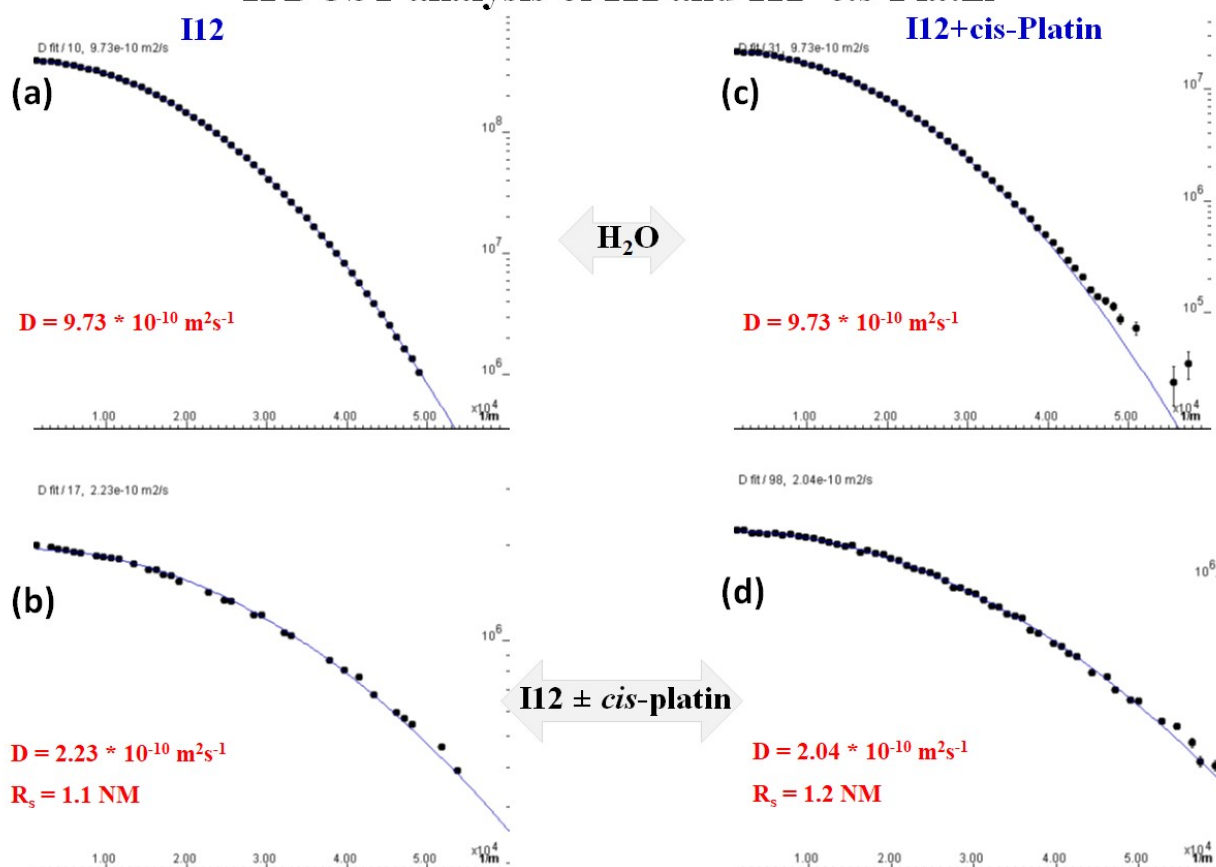


Figure S6. The quantitative analysis of diffusion data of I12 before and after the addition of *cisplatin*, the plot of rate of diffusion for (a) residual water in I12 (b) a resonance of I12 (c) residual water after the addition of *cisplatin* and (d) I12+*cisplatin*. The data was plotted using Bruker Dynamics Center 2.8.0.1 software in automation mode.

2c. Detection of conformational changes by ¹H and ¹³C NMR after the addition of *cisplatin*

Detecting the of conformational or structural changes in addition to the ligand could be direct evidence of the interaction between the studied molecule and the ligand. Such interactions could be evident in many ways by NMR spectroscopy, such as a change in chemical shift, line broadening or appearance of additional resonances in the resulting spectra.

On adding the *cisplatin* to the molecules **G12** and **I12** we could not see any substantial changes immediately in the chemical shifts of both the molecules either in ¹H or ¹³C NMR spectra. But on acquiring the spectra approximately after 6 hrs, we evident the appearance of additional resonances in the ¹H and ¹³C spectra of both the molecules **G12** and **I12**. The change in resonances is evident almost for all the resonances of ¹H spectra of the glucose

ring's proton, but the substantial difference could only be seen for the specific resonances. The 1D ^1H NMR spectra of G12 with and without cisplatin are compared in Figure S7.

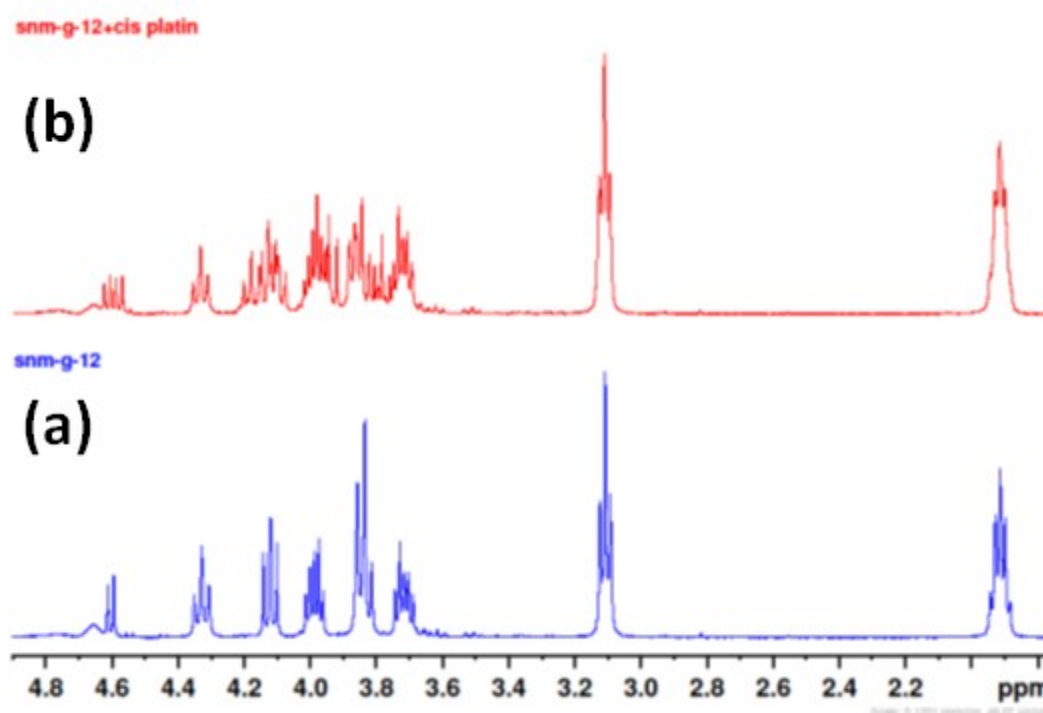


Figure S7: 1D ^1H 400 MHz NMR spectrum of (a) molecule G12 (b) the molecules G12+*cisplatin*. The appearance of additional resonances for most of the signals can be evident by comparing both the spectrum, which is more prominent for the protons of the ring, ranging from 3.6-4.6 ppm. This signal splitting is due to the interaction between G12 and *cisplatin*.

The appearance of additional signals for some ^{13}C of the ring is also obtained. To visualize these signals, the multiplicity edited by 135° pulse in ^1H - ^{13}C HSQC (heteronuclear single quantum correlation) experiment on **G12** and **I12** with and without the addition of *cisplatin* were carried out and given in Figure S8a. The multiplicity editing is advantageous in distinguishing the CH_2 resonances from the CH and CH_3 in the HSQC spectrum. The additional CH signals in ^1H - ^{13}C HSQC spectrum of G12 after the addition of cisplatin were obtained in the ^1H and ^{13}C dimension, which can be visualized in the expanded spectrum given in Figure S8b. The appearance of these additional resonances in the ^1H and ^{13}C dimensions is concluded due to the interaction between G12 and cisplatin.

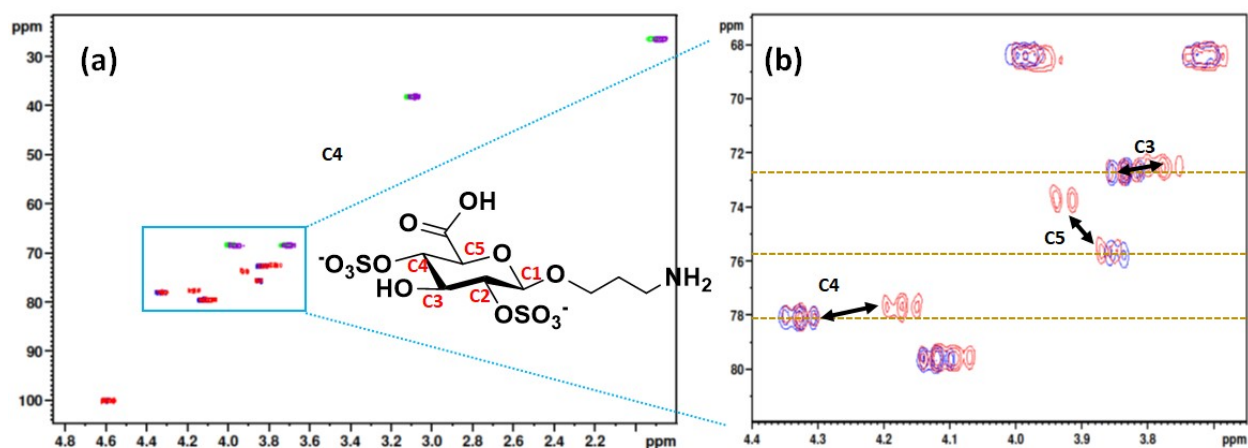


Figure S8: The stacked plot of multiplicity edited ^1H - ^{13}C HSQC (heteronuclear single quantum correlation) experiment by 135° pulse on G12 and G12+cisplatin. Blue and green contours belong to G12, and the red and purple contours to the G12+cisplatin.

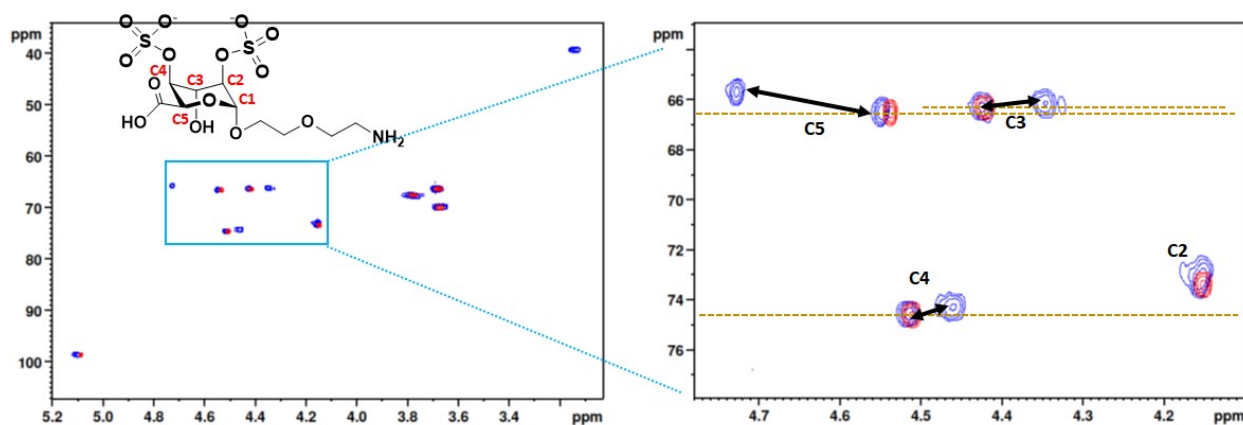


Figure S9: The stacked plot of multiplicity edited ^1H - ^{13}C HSQC (heteronuclear single quantum correlation) experiment by 135° pulse on I12 and I12+cisplatin. Blue and green contours belong to I12, and the red and purple contours to the I12+cisplatin.

Interestingly, the displacement in the newly appearing peaks is observed only for a few resonances, which is useful in identifying the most affected sites on G12 by the interaction of cisplatin. The extent of the displacement can be correlated to the effect of the interaction by cisplatin on the particular site.

The molecules G12 and I12 exist in the most stable conformer, which is probably the chair form, and after the addition of cisplatin, it shifts to the two different conformers, which may be the chair, boat, or two different kinds of twisted or any combination.

The ^1H and ^{13}C spectra also reveal information about the most affected sites by the interaction of cisplatin in the glucose molecules. As discussed, almost all ^1H resonances of the glucose ring are influenced by interaction with the cisplatin, but this change is selective for the specific sites of the backbone carbons. Few ^{13}C obtained were almost unaffected and appeared at the same chemical shift as in the free molecule; on the other hand, few ^{13}C resonances were obtained splitted and shifted in the ^{13}C dimension with different extents of shifting. The extent of displacement in the ^{13}C dimension could be used to classify the most and least affected sites on interaction with cisplatin.

The G12 and I12 were fully assigned before the interaction studies using advanced 2D NMR techniques such as COSY, ^1H - ^{13}C HSQC, ^1H - ^{13}C HMBC etc., as per the requirement. In molecule **G12**, after interaction with cisplatin, carbon C5, which is substituted with carboxylic acid, shows the maximum shift in both the ^1H and ^{13}C chemical shifts; however, C4 is the second, and the carbon C3 is the third cite on the backbone with a substantial change in their chemical shifts. This change in ^1H and ^{13}C resonances is due to the conformational change in the glucose derivatives by the interaction of cisplatin. Similar to G12, the carboxylic substituted C5 of I12 shows the maximum shift in both ^1H and ^{13}C chemical shifts, but the ^1H and ^{13}C shifts are more for C3 than C4.

Based on the above observations, it is clear that the binding site is the sulphate group on the glucose backbone; additionally, the carbonyl group at position C5 also interacts with cisplatin through hydrogen bonding. As the mode of binding in I12 is different where the sulphate groups at position C4 and C2 interact with the cisplatin by replacing its two chlorides, position C3 is most affected compared to C4. On the other hand, in G12 the cisplatin interacts with sulphate at C4, and such an effect is not prominent for position C3. The different trend in the extent of the shift in the resonances of C3 and C4 is discarding the possibility of the carbonyl group as the only interacting site with cisplatin; hence the main interaction sites are the sulphate and carboxylic groups.

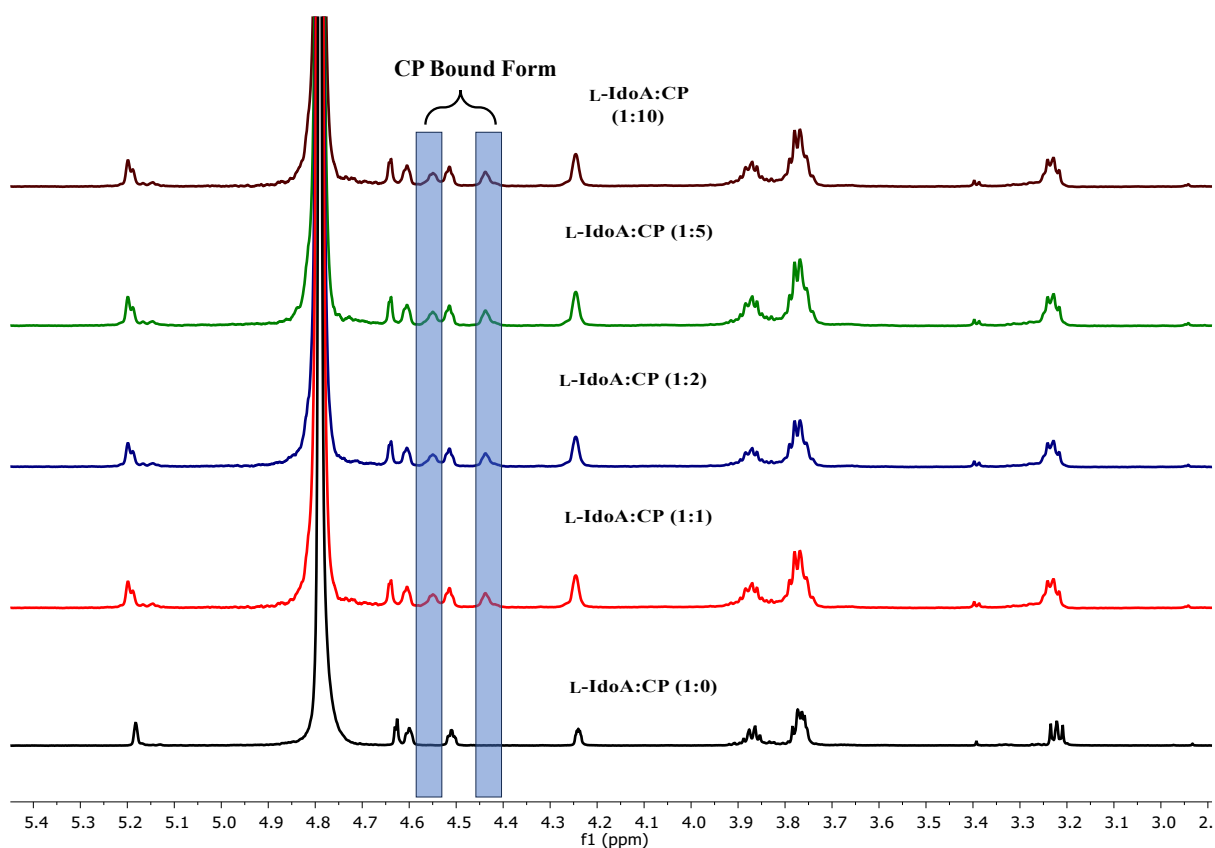


Figure S10. Quantitative NMR studies of L-IdoA with cisplatin.

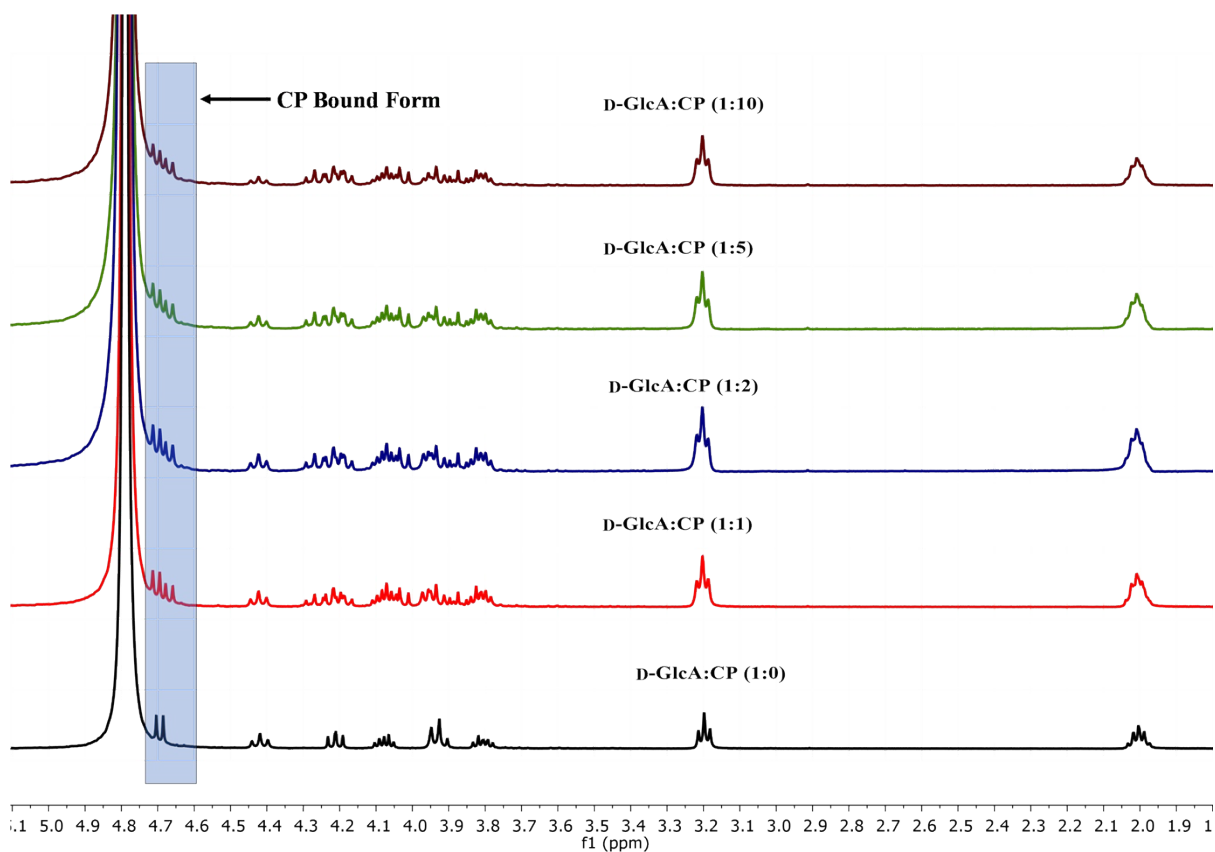


Figure S11. Quantitative NMR studies of D-GlcA with cisplatin.

A quantitative NMR investigation of L-IdoA/D-GlcA with cisplatin was conducted to determine the optimal stoichiometry of the complex. In this regard, L-IdoA/D-GlcA was mixed with cisplatin (CP) in D₂O and left in the NMR tube for one day, after which NMR measurements were taken. Figure S10 and S11 illustrates that there is no significant alteration in the NMR spectra after forming a 1:1 complex, as compared to a 1:2, 1:5, or 1:10 ratio of the complex. This suggests that the 1:1 complex is deemed ideal for further studies on complexation.

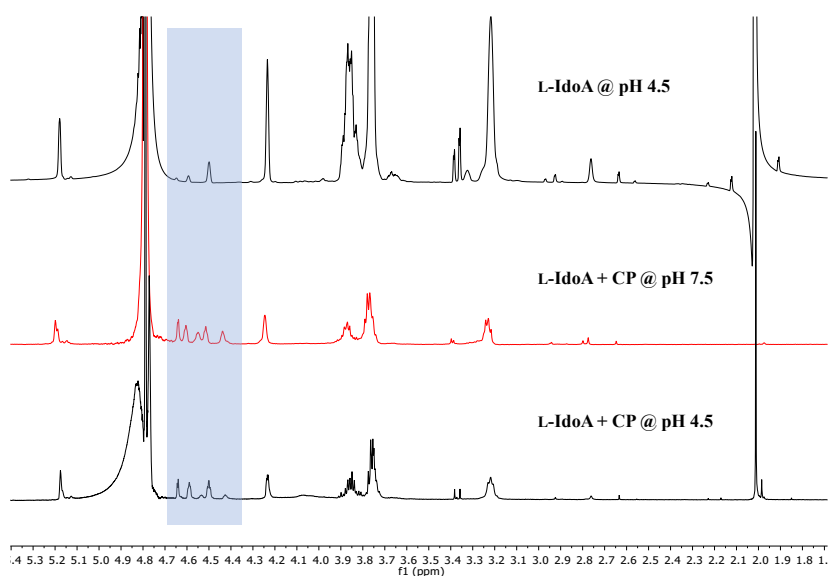


Figure S12. NMR analysis of L-IdoA-CP complex at different pH.

An investigation into the drug release mechanism was conducted at 1:1 concentration of the complex under different pH conditions. Figure S12 revealed that the complex is nearly or entirely released at pH 4.5. Conversely, at pH 7.5 and pH 5.5 (data not included as the NMR spectra appear similar to pH 7.5), no significant changes were observed in the spectra compared to the complex. Furthermore, at pH 4.5, the NMR spectra clearly indicate that the dissociation of the complex is a rapid mechanism. Consequently, determining the dissociation constant proved to be challenging.

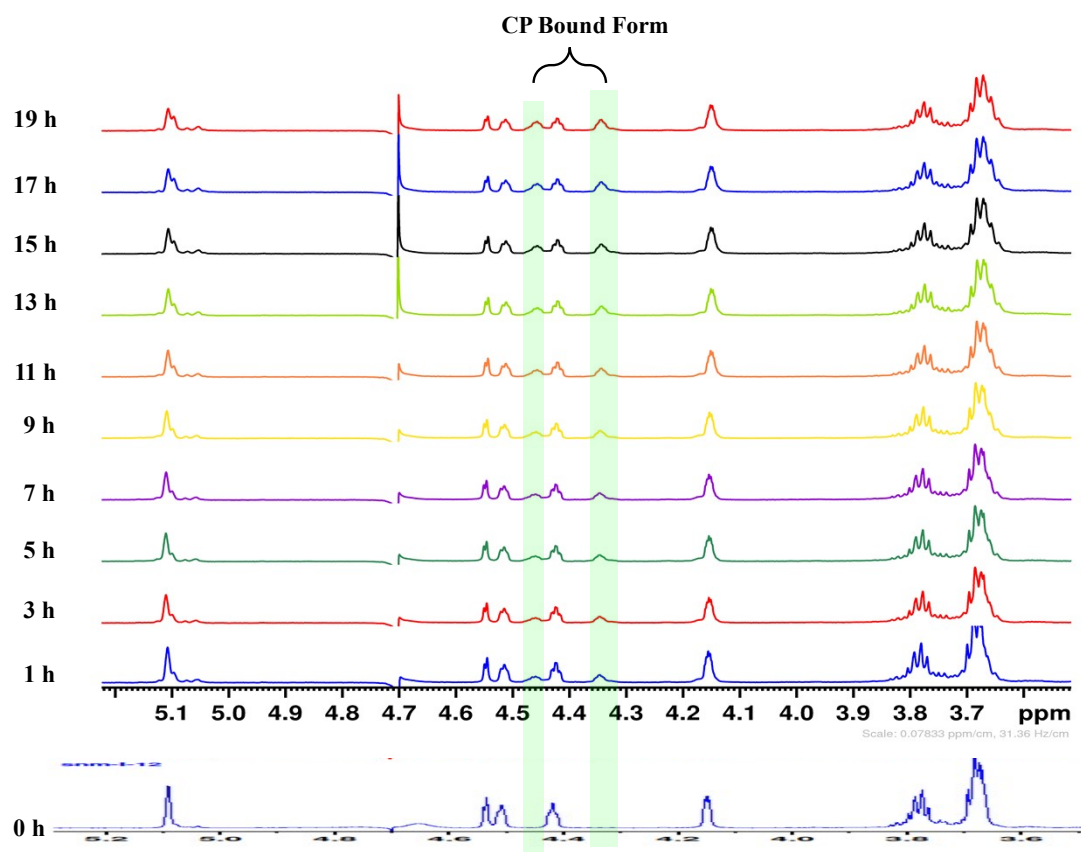


Figure S13. Time dependent complex formation between L-IdoA and CP (1:1 mixture)

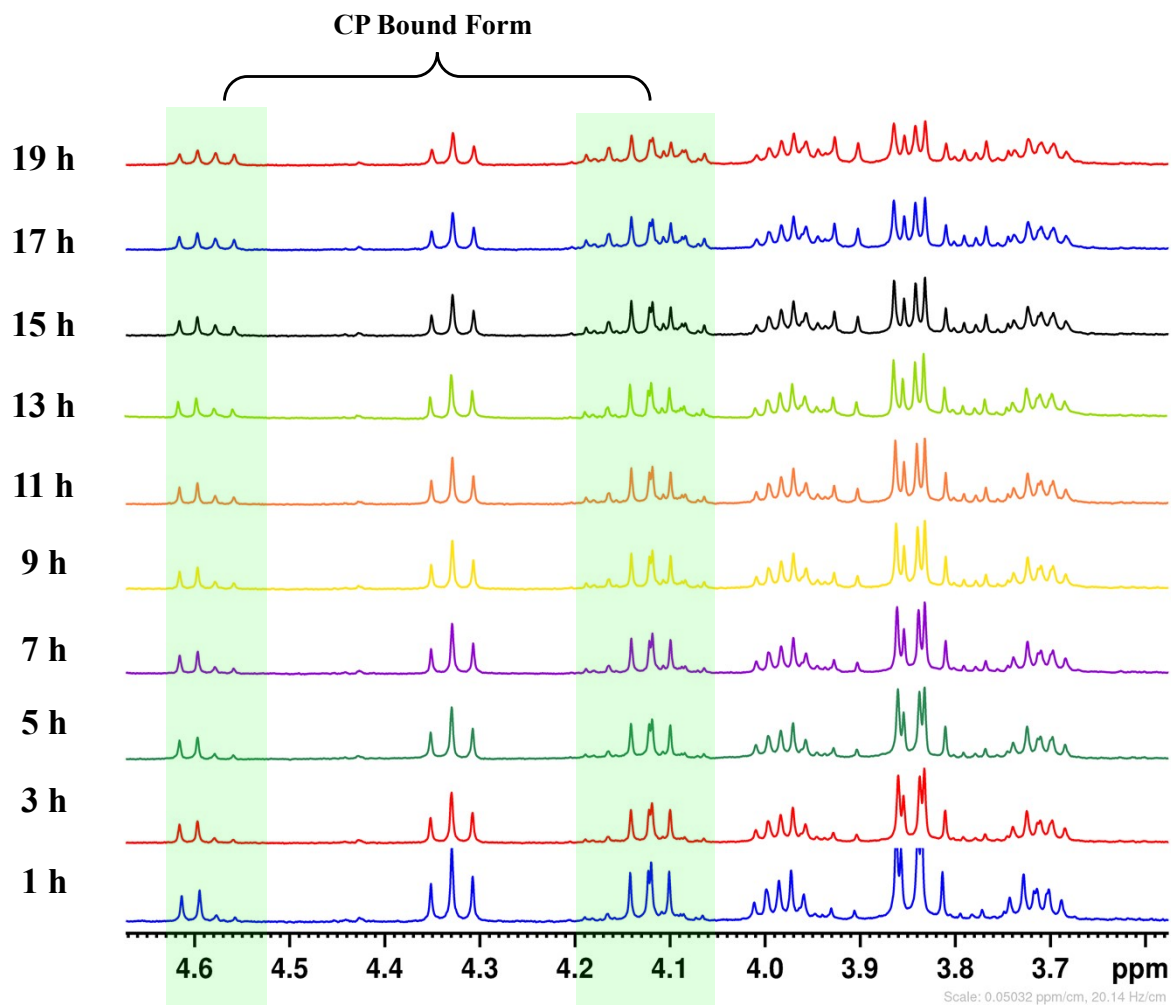


Figure S14. Time dependent complex formation between D-GlcA and CP (1:1 mixture).

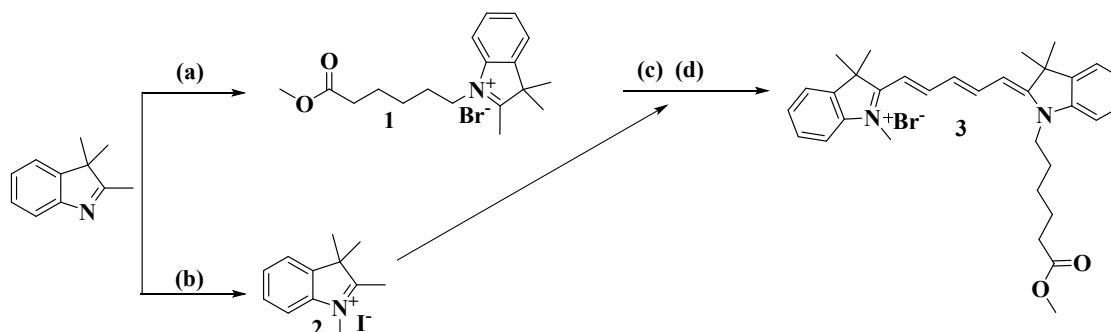
Time-dependent NMR studies were conducted with the L-IdoA/D-GlcA and cisplatin (CP) complex. Figure 13 disclosed the emergence of new peaks at 3.45 and 4.45 ppm, simultaneously with the reduction of peaks at 4.43, 4.52, and 4.55 ppm during the conformation of the L-IdoA-CP complex. Subsequent 2D-NMR analyses confirmed the binding mode (Figure S9). A similar trend was also noted in the formation of the D-GlcA-CP complex.

3. Rate of complex formation.

To determine the rate of complex formation of **G12** and **I12**, we performed kinetic studies of ligand-CP at different time intervals (0 to 48 h) and the changes in the NMR peak was

evaluated. Based on the integration value of C2 and C4 of **I12** and **G12**, rate of association was calculated.

4. Synthesis of fluorescent Probe



Scheme 1. (a) 6, 1,2- dichlorobenzene, 120 °C, 4 h (b) Methyl iodide, ACN, reflux, 7 h (c) Malonaldehyde bis(phenylimine)monohydrochloride, Acetic anhydride, reflux, 1 h (d) 7, Py., rt, 2 h

1-(6-methoxy-6-oxohexyl)-2,3,3-trimethyl-3H-indol-1-ium bromide (1)

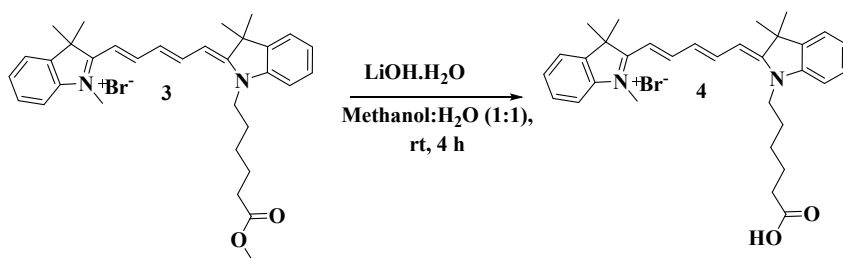
Commercially available 2,3,3-trimethyl-3H-indole (5 g, 31.4 mmol, 1 eq) and commercially available, methyl 6 – bromohexanoate (62.8 mmol, 2 eq) was dissolved in 1,2 – dichlorobenzene and it for stirring at 120 °C under nitrogen atmosphere for 4 h. After completion of reaction (~ 4 h), solvent was evaporated under reduce pressure at 52 °C. Reaction mixture was redissolved into minimum amount of cold chloroform (~5 mL), then cold acetone was added to precipitate the product. It was washed with cold acetone 3 times. After washing wine red paste of product was obtained. Yield 3.5 g (30 %). It was confirmed by HRMS. HR-ESI-MS (m/z): Calcd for $C_{18}H_{26}N_4O_2^+ [M]^+$ is 288.1958, found is 288.1956.

1,2,3,3-tetramethyl-3H-indol-1-ium iodide (2)

Commercially available 2,3,3-trimethyl-3H-indole (5 g, 31.4 mmol, 1 eq) and methyl iodide (62.8 mmol, 2 eq) was dissolved in ACN and it for stirring at 90 °C under nitrogen atmosphere for 7 h. After completion of reaction (~ 7 h), solvent was evaporated under reduce pressure. Reaction mixture was redissolved into minimum amount of cold chloroform (~5 mL), then cold acetone was added to precipitate the product. It was washed with cold acetone 3 times. After washing light maroon crystal of product was obtained. Yield 4 g (43 %). It was confirmed by HRMS. HR-ESI-MS (m/z): Calcd for $C_{12}H_{16}N^+ [M]^+$ is 174.1277, found is 174.1269.

2-((1E,3E)-5-((Z)-1-(6-methoxy-6-oxohexyl)-3,3-dimethylindolin-2-ylidene)penta-1,3-dien-1-yl)-1,3,3-trimethyl-3H-indol-1-ium iodide (3)

Compound **2** (2 g, 6.6 mmol, 1 eq) and commercially available Malonaldehyde bis(phenylimine)monohydrochloride (8 mmol, 1.2 eq) was dissolved in acetic anhydride (10 mL) and refluxed it for 1 h. After (~ 1 h), reaction mixture was cool down to rt. Then compound **1** (13.2 mmol, 2 eq) was dissolved in pyridine (15mL) followed by dropwise addition to reaction mixture at rt and stirred it 2 h. After completion of reaction (~ 2 h), solvent was evaporated under reduce pressure. After that reaction mixture was redissolved in DCM (~ 10 mL) and organic layer was washed with 10 % HCl 3 times, 3 times with 10 % NaHCO₃, 3 times with brine and dried over Na₂SO₄. The crude compound was purified through column chromatography in MeOH/ DCM (8/100) solvent system to get pure compound **9**. Yield 825 mg (21 %). ¹H NMR (400 MHz, Chloroform-d) δ 8.15 (t, J = 13.0, 2H), 7.39 – 7.30 (m, 4H), 7.23 – 7.16 (m, 2H), 7.13 – 7.02 (m, 2H), 6.83 (t, J = 12.4 Hz, 1H), 6.31 (t, J = 13.6, 2H), 4.05 (t, J = 7.6 Hz, 2H), 3.69 (s, 3H), 3.63 (s, 3H), 2.33 (t, J = 7.3 Hz, 2H), 1.86 – 1.77 (m, 3H), 1.74 (d, J = 11.5 Hz, 12H), 1.71 – 1.64 (m, 3H), 1.55 – 1.45 (m, 2H). ¹³C NMR (100 MHz, Chloroform-d) δ 173.88, 172.89, 153.83, 142.74, 142.01, 141.35, 141.02, 128.61, 128.57, 126.44, 125.17, 125.10, 122.36, 122.21, 110.49, 110.42, 104.09, 103.66, 51.60, 49.44, 49.36, 44.25, 33.68, 32.49, 28.19, 28.01, 27.13, 26.38, 24.55. HR-ESI-MS (m/z): Calcd for C₃₃H₄₁N₂O₂⁺ [M]⁺ is 497.3163, found is 497.3161.

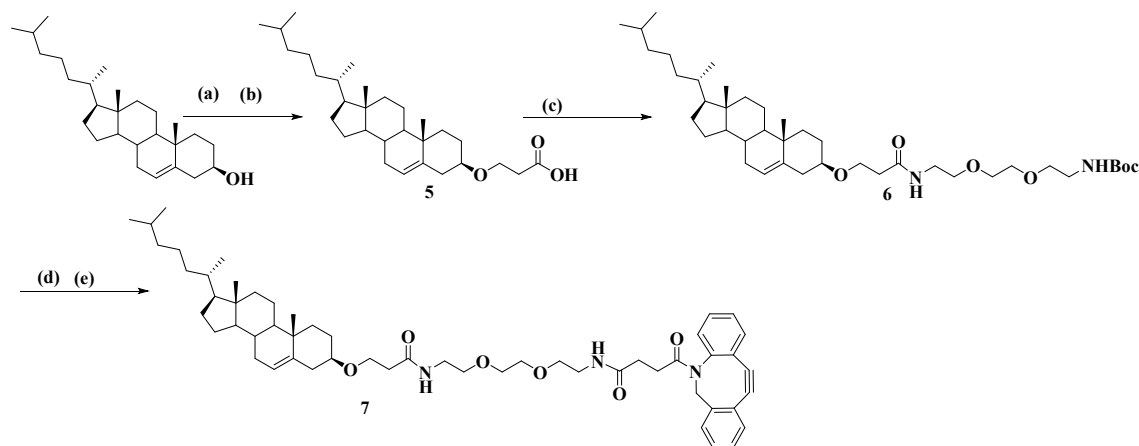


2-((1E,3E)-5-((Z)-1-(5-carboxypentyl)-3,3-dimethylindolin-2-ylidene)penta-1,3-dien-1-yl)-1,3,3-trimethyl-3H-indol-1-ium iodide (4)

Compound **4** (825 mg, 1.32 mmol, 1 eq) was dissolved in MeOH: H₂O (1:1) followed by addition of LiOH.H₂O (2.64 mmol, 2 eq) and stirred it at rt for 4 h. After completion of reaction (~ 4 h), organic solvent was evaporated under reduced pressure. Then the aqueous layer was washed with DCM 3 times (~ 30 mL) and later the organic layer was washed 10 % HCl 3 times (~ 50 mL), 3 times with brine and dried over Na₂SO₄. The crude compound was

purified through column chromatography in MeOH/ DCM (1/10) solvent system to get pure compound **10**. Yield 757 mg (94 %). ¹H NMR (400 MHz, Chloroform-d) δ 7.90 (t, J = 13.0, 2H), 7.41 – 7.27 (m, 4H), 7.21 – 7.13 (m, 2H), 7.07 (dd, J = 13.0, 7.9 Hz, 2H), 6.93 (t, J = 12.5 Hz, 1H), 6.54 (d, J = 13.6 Hz, 1H), 6.38 (d, J = 13.6 Hz, 1H), 4.01 (t, J = 7.7 Hz, 2H), 3.68 (s, 3H), 2.52 (t, J = 7.0 Hz, 2H), 1.78 (m, 5H), 1.67 (d, J = 3.4 Hz, 12H), 1.55 (m, 2H). ¹³C NMR (101 MHz, Chloroform-d) δ 173.5, 172.8, 153.7, 153.7, 142.8, 142.0, 141.2, 141.0, 128.8, 128.7, 126.4, 125.2, 122.3, 122.2, 110.7, 110.6, 104.2, 103.7, 77.6, 77.3, 76.9, 50.3, 49.4, 49.3, 44.2, 34.7, 32.0, 31.9, 30.4, 29.7, 29.7, 28.1, 28.0, 26.8, 26.3, 24.5, 14.2. HR-ESI-MS (m/z): Calcd for C₃₂H₃₉N₂O₂⁺ [M]⁺ is 483.3006, found is 483.2998.

5. Synthesis of cholesterol linker



Scheme 2. (a) *tert*-butyl acrylate, NaH, THF, rt, 16 h (b) 40 % TFA in DCM, rt, 2 h (c) *tert*-butyl (2-(2-(2-aminoethoxy)ethoxy)ethyl)carbamate, DCC, DCM, 0 °C, 12 h (d) 40 % TFA in DCM, rt, 2 h (e) NHS – DBCO, NEt₃, DCM, rt, 12 h.

3-(((3R,10S,13S,17S)-10,13-dimethyl-17-((S)-6-methylheptan-2-yl)-2,3,4,7,8,9,10,11,12,13,14,15,16,17-tetradecahydro-1H-cyclopenta[a]phenanthrene-3-yl)oxy)propanoic acid (**5**)

Commercially available cholesterol (5 g, 12.9 mmol, 1 eq) was dissolved in 50 mL of THF, then NaH (181 mmol, 14 eq) was added in 4 portions. After that *tert*-butyl acrylate (3.9 mmol, 0.3 eq) was dissolved in 20 mL of THF and addition was done in dropwise manner. The progress of reaction was monitored by TLC. After completion of reaction (~ 16 h), reaction was quenched by addition of 15 mL of MeOH and solvent was evaporated under reduce pressure. Then reaction mixture was redissolved in DCM and it's washed with 10 % HCl 3 times, 3 times with brine and dried over Na₂SO₄. The crude compound was purified

through column chromatography in ethyl acetate / hexane (4/10) solvent system to get pure compound. Yield 1.1 g (55 %). After that, product (1.1 g, 2.2 mmol, 1 eq) was dissolved in 40 % TFA in DCM and stirred it for 2 h at rt. The progress of reaction was monitored by TLC. After completion of reaction (~ 2 h), solvent was evaporated under reduce pressure. Then reaction mixture was redissolved into DCM (~ 50mL) and its's washed with 10 % NaHCO₃ 3 times, 3 times with brine and dried over Na₂SO₄. The crude compound was purified through column chromatography in ethyl acetate / hexane (6/10) solvent system to get pure compound **5**. Yield 897 mg (90 %). ¹H NMR (400 MHz, Chloroform-d) δ 5.35 – 5.34 (m, 1H), 3.76 (t, J = 6.3, 2H), 3.20 (m, 1H), 2.62 (t, J = 6.3 Hz, 2H), 2.39 – 2.34 (m, 1H), 2.24 – 2.13 (m, 1H), 2.06 – 1.93 (m, 2H), 1.92 – 1.76 (m, 3H), 1.62 – 1.42 (m, 7H), 1.41 – 1.23 (m, 5H), 1.22 – 1.01 (m, 8H), 0.99 (s, 4H), 0.91 (d, J = 6.6 Hz, 3H), 0.86 (dd, J = 6.6, 1.8 Hz, 6H), 0.67 (s, 3H). ¹³C NMR (101 MHz, CHLOROFORM-D) δ 176.6, 140.7, 121.9, 79.7, 77.4, 77.1, 76.8, 63.1, 56.8, 56.2, 50.2, 42.4, 39.9, 39.6, 39.0, 37.2, 36.9, 36.3, 35.9, 35.3, 32.0, 32.0, 28.3, 28.3, 28.1, 24.4, 23.9, 22.9, 22.7, 21.1, 19.5, 18.8, 11.9, 0.1. HR-ESI-MS (m/z): Calcd for C₃₀H₅₀O₃ [M] is 458.3760, found is 458.3759.

N-(2-(2-(2-aminoethoxy)ethoxy)ethyl)-3-(((3R,10S,13S,17S)-10,13-dimethyl-17-((S)-6-methylheptan-2-yl)-2,3,4,7,8,9,10,11,12,13,14,15,16,17-tetradecahydro-1H-cyclopenta[a]phenanthren-3-yl)oxy)propenamide (6)

Compound **5** (897 mg, 1.9 mmol, 1 eq) was dissolved in 10 mL of DCM. Then, DCC (2.9 mmol, 1.5 eq) and tert-butyl (2-(2-(2-aminoethoxy)ethoxy)ethyl) carbamate (2.9 mmol, 1.5 eq) was added at 0 °C under nitrogen atmosphere. The progress of reaction was monitored by TLC. After completion of reaction (~ 12 h), solvent was evaporated under reduced pressure. The crude compound was purified through column chromatography in ethyl acetate / hexane (8/10) solvent system to get pure compound. Yield 1.1 mg (80 %). ¹H NMR (400 MHz, Chloroform-d) δ 6.85 (s, 1H), 5.29 (d, J = 5.1 Hz, 1H), 5.09 (t, J = 5.8 Hz, 1H), 3.68 (t, J = 5.9 Hz, 2H), 3.56 (s, 4H), 3.53 – 3.48 (m, 4H), 3.42 (q, J = 5.2 Hz, 2H), 3.27 (q, J = 5.4 Hz, 2H), 3.18 – 3.10 (m, 1H), 2.42 (t, J = 5.8 Hz, 2H), 2.33 – 2.28 (m, 1H), 2.17 – 2.10 (m, 1H), 1.98 – 1.72 (m, 5H), 1.51 – 1.42 (m, 5H), 1.39 (s, 12H), 1.34 – 1.24 (m, 3H), 1.23 – 1.19 (m, 2H), 1.12 – 1.05 (m, 4H), 1.04 – 0.97 (m, 3H), 0.95 (s, 3H), 0.87 (d, J = 6.5 Hz, 3H), 0.81 (dd, J = 6.6, 1.8 Hz, 6H), 0.63 (s, 3H). ¹³C NMR (101 MHz, CDCl₃) δ 172.0, 156.0, 140.5, 121.9, 79.4, 77.4, 77.1, 76.8, 70.2, 70.1, 69.8, 63.9, 56.7, 56.1, 50.1, 42.3, 40.3, 39.7, 39.5, 39.1, 39.0, 37.2, 37.1, 36.8, 36.2, 35.8, 31.9, 31.8, 28.4, 28.3, 28.2, 28.0, 24.3, 23.8, 22.8,

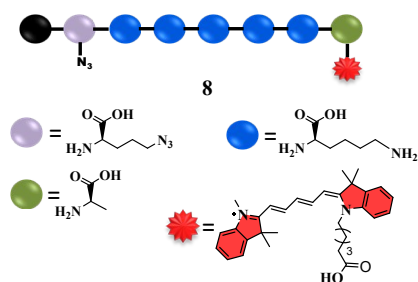
22.5, 21.0, 19.4, 18.7, 11.8. HR-ESI-MS (m/z): Calcd for C₄₁H₇₂N₂O₆ [M] is 688.5390, found is 688.5381.

Synthesis of compound 7:

After that Boc group was deprotected using 40 % TFA in DCM. The crude compound was purified by column chromatography ethyl acetate/ hexane (8/10). Yield 844 mg (90 %). Compound **6** (6 mg, 50.9 μmol, 1 eq) was dissolved in DCM followed by dropwise addition of NEt₃ (56 μmol, 1.1 eq). After that NHS – DBCO (45.8 μmol, 0.9 eq) was added and stirred for 12 h at rt. The progress of reaction was monitored using TLC. After completion of reaction (~12 h), solvent was evaporated under reduce pressure. The crude compound was purified through column chromatography in ethyl acetate/ hexane (1/2) solvent system to get pure compound **7**. Yield 8.1 mg (94 %). ¹H NMR (400 MHz, Chloroform-d) δ 7.66 (d, J = 7.3 Hz, 1H), 7.55 – 7.43 (m, 1H), 7.41 – 7.26 (m, 5H), 7.25 (d, J = 1.7 Hz, 1H), 6.81 (t, J = 5.6 Hz, 1H), 6.26 (t, J = 5.5 Hz, 1H), 5.35 – 5.29 (m, 1H), 5.14 (d, J = 13.9 Hz, 1H), 3.74 – 3.62 (m, 3H), 3.62 – 3.50 (m, 6H), 3.49 – 3.37 (m, 4H), 3.33 (dd, J = 5.7, 4.1 Hz, 2H), 3.20 – 3.12 (m, 1H), 2.84 – 2.77 (m, 1H), 2.48 – 2.38 (m, 3H), 2.36 – 2.30 (m, 1H), 2.19 – 2.14 (m, H), 2.07 – 1.75 (m, 8H), 1.63 – 1.28 (m, 9H), 1.25 (s, 3H), 1.19 – 0.97 (m, 6H), 0.97 (s, 3H), 0.91 (d, J = 6.5 Hz, 3H), 0.86 (dd, J = 6.6, 1.8 Hz, 6H), 0.66 (s, 3H). ¹³C NMR (101 MHz, CDCl₃) δ 171.2, 170.8, 161.4, 150.3, 147.1, 131.2, 128.4, 127.7, 127.2, 127.1, 126.7, 126.0, 124.5, 122.2, 121.4, 120.8, 117.3, 114.4, 113.6, 106.9, 76.4, 76.1, 75.8, 63.0, 55.7, 55.1, 54.5, 51.6, 49.1, 41.3, 38.7, 38.5, 38.1, 38.0, 36.1, 35.8, 35.2, 34.8, 30.9, 30.2, 29.2, 28.7, 27.2, 27.0, 24.3, 23.3, 22.8, 21.8, 21.5, 20.0, 18.4, 17.7, 10.8, 7.5, 6.5. Calcd for C₅₅H₇₇N₃O₆ [M] is 875.5812, found is 875.5801.

6. Synthesis of neoproteoglycan (P-I12)

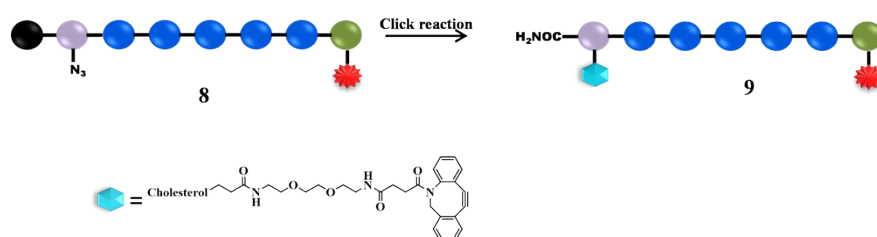
Synthesis of compound 8:



Compound **8** was synthesized through a manual solid phase peptide synthesis on rink amide resin at 0.3 mmol scale using standard Fmoc- conditions. The combination of HBTU and

HOBt was used as coupling reagents, DIPEA was used as an activator base, NMP was used as a coupling solvent and 20% piperidine in DMF was used for the Fmoc- group deprotection. To release the peptides from the solid support, the resin was stirred for about 2 hours in a 10 mL cocktail containing trifluoroacetic acid (TFA)/triisopropylsilane/water/phenol (90:5:2.5:2.5). The resin was filtered. The filtrate containing crude peptides was evaporated under reduced pressure and the residue was triturated with cold diethyl ether (20 mL). The precipitate was separated through centrifugation. The crude peptides were again dissolved in 10 mL of MeOH and purified on a C18 column using reversed-phase HPLC. MeOH and water gradient system containing 0.1% of TFA at a 1 ml flow rate was used to purify the peptides. The purified peptides was confirmed by IR, NMR and HR-ESI-MS Calcd for C₇₀H₁₁₃N₁₈O₈⁺ [M] is 1334.5291, found is 1334.5280. ¹H NMR (400 MHz, Acetonitrile-d₃) δ 8.21 (t, J = 13.1 Hz, 2H), 8.15 – 7.92 (m, 7H), 7.75 – 7.63 (m, 11H), 7.61 (m, 3H), 7.55 (m, 2H), 7.39 (t, J = 7.4 Hz, 4H), 6.68 (t, J = 12.4 Hz, 1H), 6.34 (dd, J = 13.8, 5.2 Hz, 2H), 4.36 (m, 8H), 4.14 (t, J = 7.5 Hz, 4H), 3.68 (s,3H), 3.11 (m, 2H), 3.06 (m, 10H), 2.37 (t, J = 7.5 Hz, 2H), 2.11 (p, J = 2.5 Hz, 2H), 1.98 – 1.82 (m,11H), 1.81 (s, 12H), 1.79 – 1.69 (m, 13H), 1.61 – 1.46 (m, 11H), 1.45 – 1.41 (m, 3H). ¹³C NMR (151 MHz, Acetonitrile-d₃) δ 175.9, 175.1, 174.7, 174.0, 173.3, 161.7, 154.8, 154.7, 143.9, 143.2, 142.3, 142.2, 129.6, 129.4, 129.4, 126.0, 125.8, 125.4, 123.1, 123.0, 118.4, 118.3, 118.1, 116.9, 115.4, 111.7, 111.7, 104.0, 103.6, 56.2, 53.6, 51.6, 51.0, 50.3, 50.1, 50.0, 49.8, 49.7, 49.2, 49.1, 49.0, 49.0, 48.8, 48.7, 48.5, 48.4, 47.7, 45.8, 44.7, 43.2, 40.1, 35.9, 31.7, 31.2, 30.8, 30.7, 30.7, 29.6, 27.7, 27.6, 27.4, 27.0, 26.0, 25.8, 23.2, 23.2, 17.1.

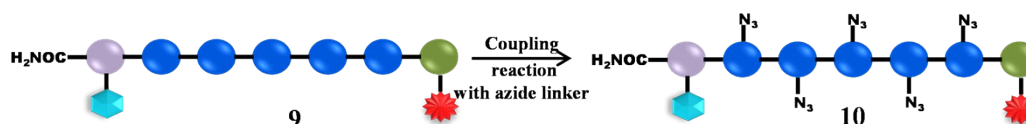
Synthesis of compound 9:



Compound **8** (12 mg, 0.009 mmol, 1 eq) was dissolved in 500 μ L of MeOH and compound **7** (0.009 mmol, 1 eq) was dissolved in 500 μ L of DCM, followed by dropwise addition of compound **8** solution into compound **7** solution and kept it stirring for 12 h at rt. The progress of reaction was monitored by MALDI-TOF/TOF analysis. After completion of reaction (~ 12 h), solvent was evaporated under reduced pressure. The crude compound was purified through C-18 bond elute column chromatography in MeOH/ H₂O (6/10) solvent system to get

pure compound **9**. It was confirmed by IR, NMR and HR-ESI-MS Calcd for $C_{125}H_{190}N_{21}O_{14}^+$ [M] is 2209.4796, found is 2210.4816 (M+H). 1H NMR (400 MHz, Methanol-d₄) δ 8.26 (t, J = 13.0, Hz, 2H), 8.00 – 7.80 (m, 1H), 7.72 – 7.54 (m, 4H), 7.51 -7.49(m, 2H), 7.46 – 7.34 (m, 4H), 7.34 – 7.20 (m, 6H), 6.62 (t, J = 12.4 Hz, 1H), 6.29 – 6.26 (d, J = 13.8Hz, 2H), 5.35 (d, J = 4.9 Hz, 1H), 4.63 – 4.20 (m, 14H), 4.17 – 4.07 (m, 2H), 3.75 – 3.70 (m, 2H), 3.63 (s, 3H), 3.60 (d, J = 5.9 Hz, 3H), 3.56 – 3.48 (m, 4H), 3.38 – 3.35 (m, 3H), 3.19 – 3.13 (m, 1H), 2.98 – 2.89 (m, 10H), 2.44 – 2.27 (m, 7H), 2.17 – 1.81 (m, 17H), 1.73 (s, 12H), 1.71 – 1.62 (m, 15H), 1.57 – 1.42 (m, 19H), 1.40 – 1.29 (m, 10H), 1.21 – 1.03 (m, 8H), 1.00 (s, 3H), 0.94 (d, J = 6.5 Hz, 3H), 0.88 (dd, J = 6.6, 1.4 Hz, 6H), 0.72 (s, 3H). ^{13}C NMR (151 MHz, Methanol-d₄) δ 174.8, 174.2, 173.1, 172.8, 161.7, 161.5, 154.3, 154.0, 142.8, 142.2, 141.2, 141.1, 140.5, 128.4, 125.2, 125.0, 124.8, 122.1, 121.9, 121.4, 117.8, 115.9, 110.5, 103.1, 102.7, 79.2, 69.9, 69.2, 63.7, 56.8, 56.2, 53.4, 50.3, 49.2, 49.1, 48.2, 48.0, 47.9, 47.7, 47.6, 47.5, 47.3, 47.2, 43.4, 42.1, 39.7, 39.3, 39.1, 38.8, 37.0, 36.6, 36.6, 36.0, 35.7, 35.0, 31.8, 31.6, 30.8, 30.1, 28.1, 27.9, 27.8, 26.9, 26.6, 26.4, 26.1, 25.1, 23.9, 23.5, 22.4, 21.8, 21.5, 20.8, 18.5, 17.8, 16.3, 16.0, 10.9.

Synthesis of compound **10** :-



Scheme 3. (a) DMF, DIPEA, rt, 16 h

Compound **9** (8 mg, 0.0036 mmol, 1 eq) was dissolved in 200 μ L of DMF and 20 μ L of DIPEA was added. Also, the 2,5-dioxopyrrolidin-1-yl 3-azidopropanoate (0.15 mmol, 50 eq) was dissolved in 200 μ L of DMF, followed by dropwise addition into compound **9** solution and kept it stirring for 12 h at rt. The progress of reaction was monitored by MALDI-TOF/TOF analysis. After completion of reaction (~ 12 h), solvent was evaporated under reduced pressure. The crude compound was purified through LH – 20 size exclusion column chromatography using MeOH as a solvent system and also passed through Amberlite® IRC120, Na⁺ form to get pure compound **10**. It was confirmed by IR, NMR and HR-ESI-MS Calcd for $C_{140}H_{205}N_{36}O_{19}^+$ [M] is 2694.6176, found is 2694.6153. 1H NMR (600 MHz, Methanol-d₄) δ 8.36 – 8.20 (m, 1H), 7.78 – 7.73 (m, 4H), 7.60 – 7.45 (m, 4H), 6.45 – 6.17 (m, 1H), 5.57 (d, J = 5.1, 1H), 4.40 – 4.26 (m, 8H), 4.11 – 3.96 (m, 8H), 3.93 – 3.89 (m, 7H), 3.86 – 3.82 (m, 9H), 3.81 – 3.76 (m, 12H), 3.44 – 3.38 (m, 8H), 3.12 – 3.05 (m, 14H), 2.94

(s, 10H), 2.89 – 2.75 (m, 10H), 2.70 – 2.56 (m, 19H), 2.50 – 2.46 (m, 2H), 2.41 – 2.18 (m, 6H), 2.14 – 2.05 (m, 10H), 1.97 – 1.93 (m, 10H), 1.80 – 1.72 (m, 10H), 1.70 – 1.57 (m, 16H), 1.52 – 1.50 (m, 8H), 1.42 – 1.23 (m, 9H), 1.18 – 1.14 (m, 3H), 1.11 – 1.09 (m, 6H), 0.32 (s, 3H). ¹³C NMR (151 MHz, MeOD) δ 175.2, 174.2, 173.3, 171.8, 162.6, 143.3, 142.6, 141.7, 141.5, 141.1, 126.0, 125.8, 122.9, 122.7, 122.4, 111.3, 80.1, 78.4, 78.2, 78.0, 70.7, 70.4, 70.2, 65.8, 64.5, 63.6, 57.4, 56.8, 55.0, 54.8, 54.5, 50.8, 49.9, 49.4, 49.3, 49.1, 49.0, 48.9, 48.7, 48.6, 48.1, 44.3, 42.9, 40.4, 40.1, 39.7, 39.5, 37.7, 37.5, 37.4, 37.0, 36.7, 36.4, 35.9, 34.6, 32.5, 32.5, 32.3, 31.5, 30.6, 30.2, 30.1, 30.0, 29.9, 29.8, 29.6, 29.6, 28.8, 28.8, 28.6, 28.5, 28.1, 28.0, 26.0, 25.8, 25.4, 24.8, 24.3, 23.2, 23.1, 22.8, 21.6, 19.7, 19.1, 17.2, 14.3, 12.2, 1.4, 0.1.

Synthesis of compound P-I12 (11):



Compound **10** (2 mg, 0.00074 mmol, 1 eq.) was dissolved in 200 μ L of CHCl_3 and the solution of compound **112** (0.0037 mmol, 5 eq.) in H_2O (200 μ L) was added, after that 400 μ L of MeOH was added and stirred the solution at rt for 16 h. The progress of reaction was monitored by HRMS. After completion of reaction (\sim 16 h), solvent was evaporated under reduce pressure. The crude product was purified by using 3 kDa centrifuge filter followed by C18 column using reversed-phase HPLC. ACN and water gradient system at a 1 ml flow rate was used to purify the compound **10**. It was confirmed by IR, NMR and HR-ESI-MS Calcd for $\text{C}_{285}\text{H}_{365}\text{N}_{46}\text{O}_{99}\text{S}_{10}^{9-}$ [m/z] is 704.2248, found is 704.2175. ¹H NMR (600 MHz, Deuterium Oxide) δ 7.83 (m, 2H), 7.11 (t, 41H), 5.96 (m, 5H), 5.70 (s, 4H), 5.02 (s, 4H), 4.65 (s, 7H), 4.45 (m, 10H), 4.28 (m, 5H), 4.14 (m, 5H), 3.76 – 3.64 (m, 6H), 3.63 – 3.33 (m, 41H), 3.16 (m, 20H), 2.89 (m, 18H), 2.64 – 2.44 (m, 5H), 2.32 (m, 4H), 2.25 – 1.79 (m, 24H), 1.48 (m, 20H), 1.16 (s, 63H), 0.74 (m, 2H), 0.32 (m, 24H).

7. Cell surface engineering studies:

To perform cell surface engineering studies 2×10^4 cells were plated in 8 well microscopy plates and incubated overnight. Next day different concentrations of **P-I12** were added and cells were incubated for different time intervals. On completion of incubation, cells washed with PBS and taken for imaging.

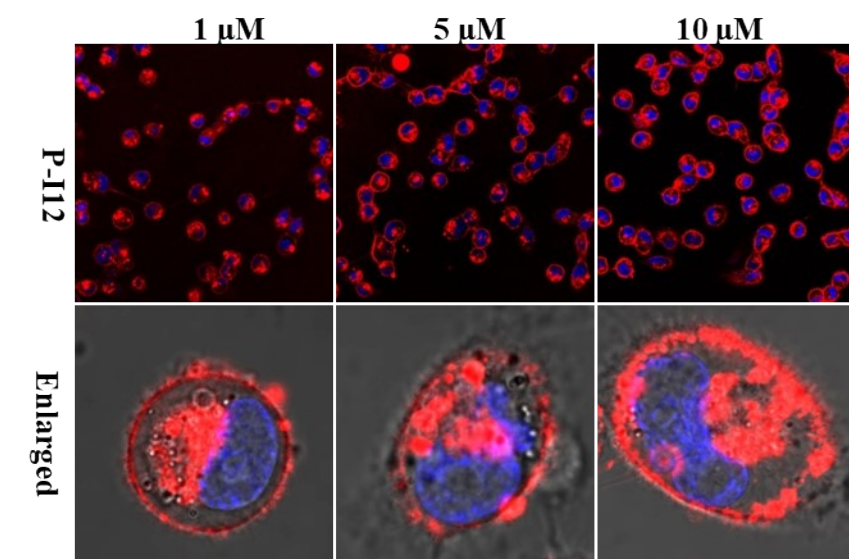


Figure S15: Confocal images of **P-I12** internalization at different concentration by MBD-MB 468 cell lines after 1 h (scale bar: 20 mm and 60 μ m).

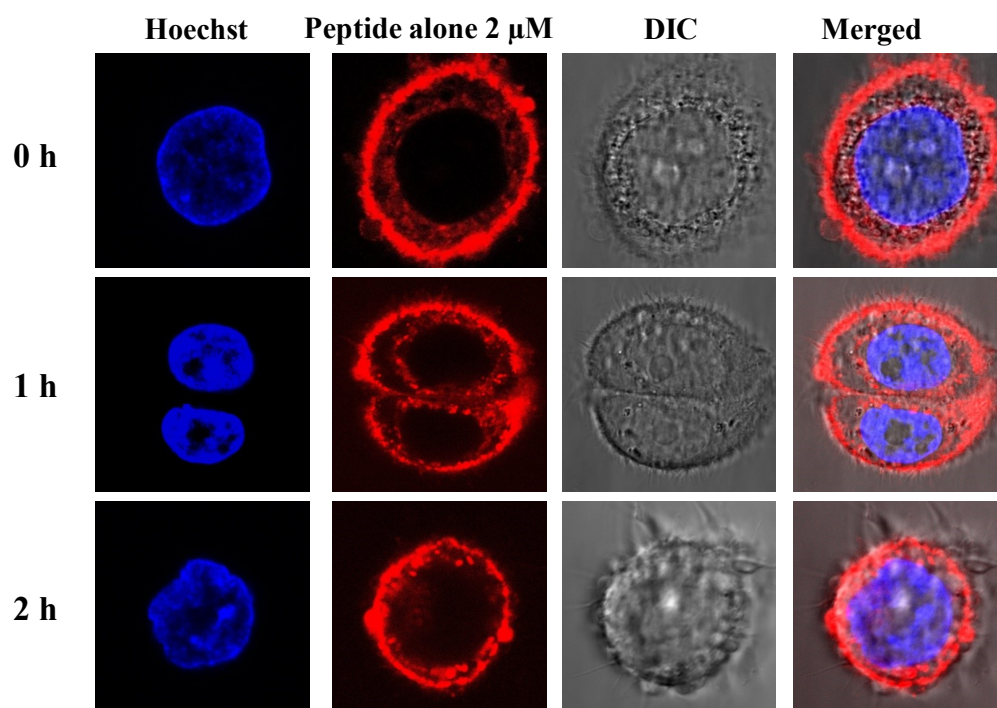


Figure S16. Confocal imaging of peptide alone on the MDA-MB-468 at different time interval.

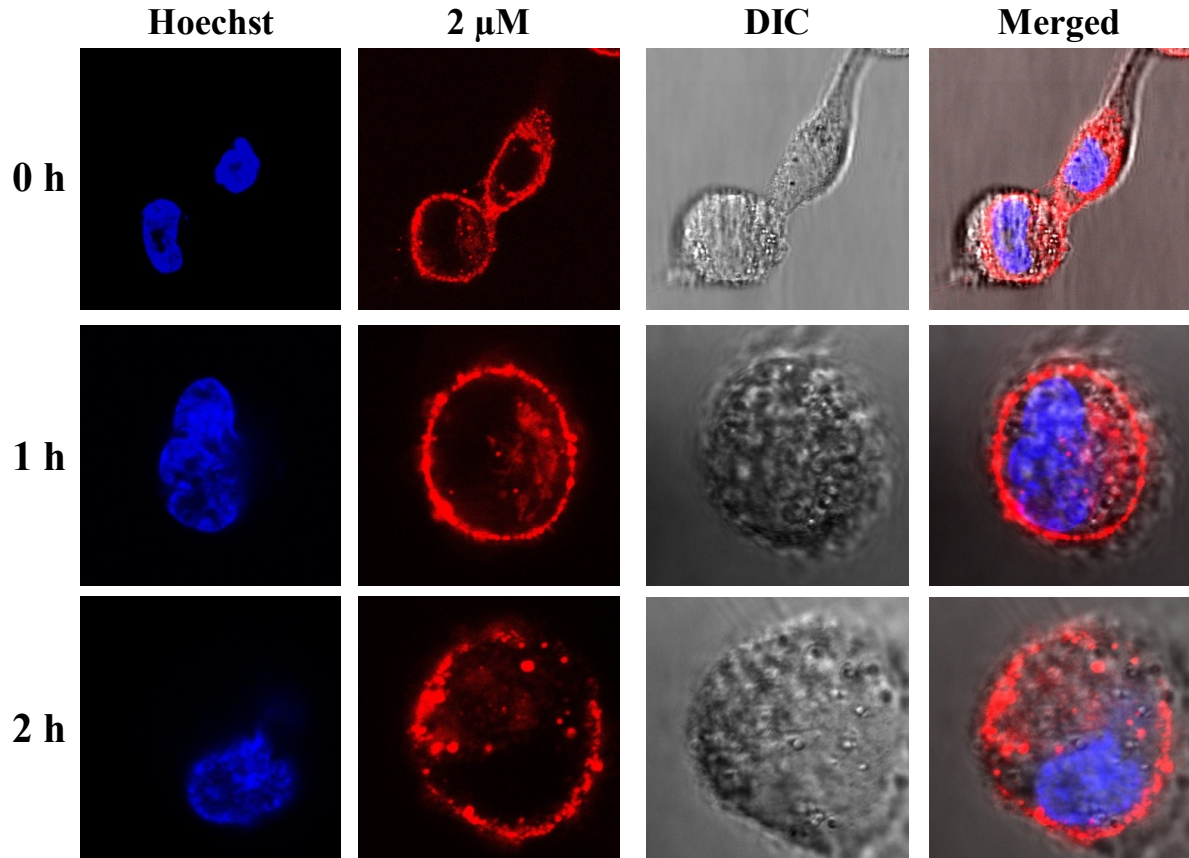


Figure S17. Confocal imaging of peptide alone on the NIH-3T3 at different time interval.

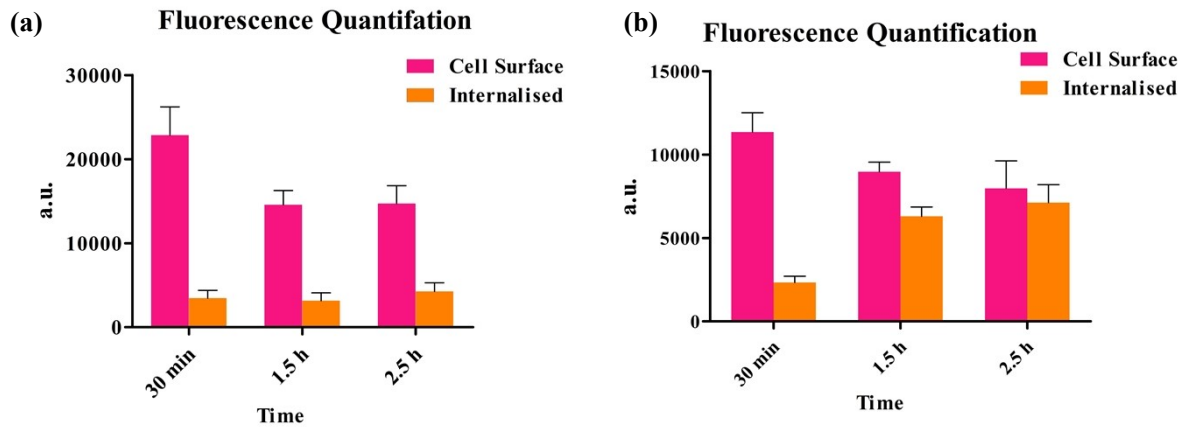


Figure S18. Quantification of peptide alone with (a) MDA-MB-468 (b) NIH-3T3 at different time interval.

Confocal imaging experiments were carried out with the peptide alone with MDA-MB-468 and NIH-3T3, revealing that the peptide gracefully decorated the membrane of both normal and cancer cells for more than 2 hours (see Figure S15, S16 and S17) and exhibited minimal internalization. These investigations distinctly revealed that the inclusion of L-idoA on the

peptides facilitated precise adjustment of cell-surface engineering on both cancer and normal cells, thereby influencing the release of cisplatin.

8. Co-localization studies:

To study cellular co-localization of IdA-paprtide conjugated cisplatin complex MDA-MB 468 cells were grown on cover glass (1×10^4 cells per well) overnight. Cells treated with $10 \mu\text{M}$ P-I12@CP for different time intervals (15 min to 24 h), followed by treatment with markers of different organelles. For lysosome labelling cells treated with lyso green for 1 h at 37°C followed by staining with Hoechst for 10 min and proceeded further for fixation with 4% paraformaldehyde and mounting of glass slides.

For early and late endosome co-localization cells first fixed using 4% paraformaldehyde then permeabilized with 0.1% triton X100 for 10 min followed by blocking with 2% BSA for 45 min at RT. Then cells labelled with primary EEA1 and LAMP2 antibody overnight at 4°C followed by washing with PBS and treatment with secondary antibody at 1:2000 dilution for 45 min at RT. Coverslips washed and mounted on glass slides for imaging.

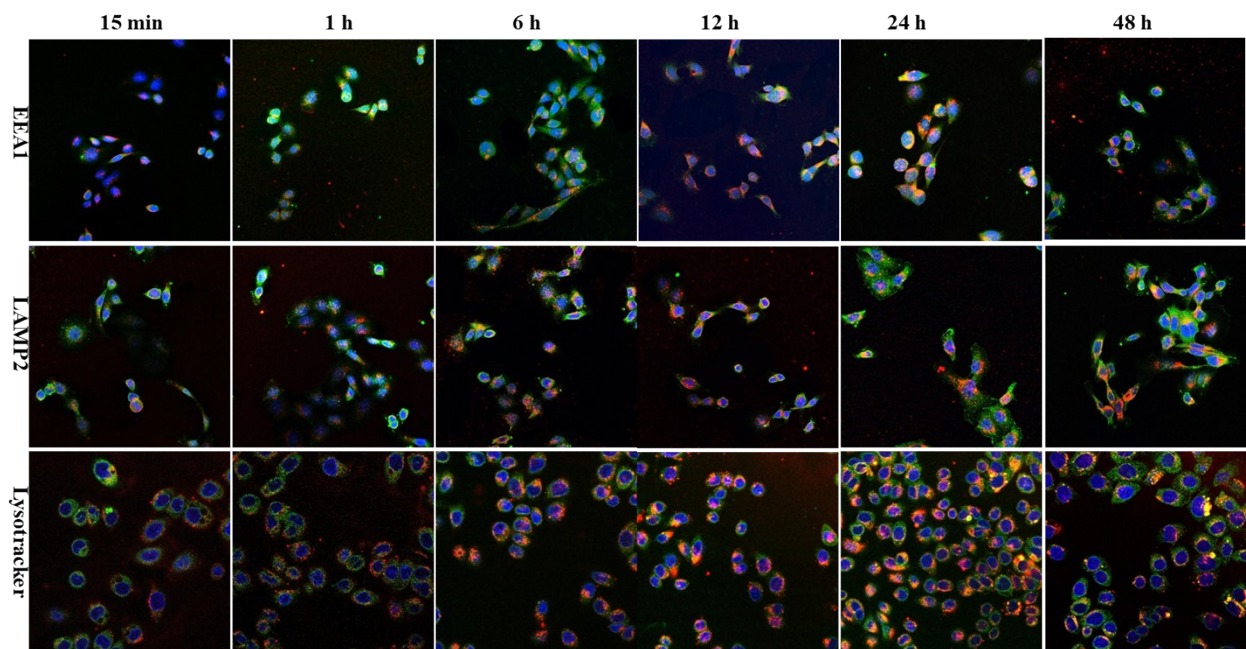


Figure S19. Confocal microscopic images for trafficking of P-I12 (red) in early (EEA1 antibody), late (LAMP2 antibody) endosome and lysosomal compartments of MDA-MB-468 cells.

9. Pathway Study:

To examine the endocytosis mechanism, we initially assessed its energy-dependent pathway. MDA-MB-468 cells were incubated with NaN₃ for 30 minutes to deplete ATP, followed by treatment with P-I12 for 2 hours. No reduction in cellular uptake of MGDs was observed, confirming that the endocytic pathway is independent of energy. To investigate the involvement of dynamin-dependent uptake, dynasore hydrate was introduced. However, no blockade of uptake was observed, indicating that internalization is not dependent on clathrin- or caveolae-mediated pathways. Similarly, the addition of methyl-β--cyclodextrin (m-β-CD, an inhibitor of caveolae-mediated endocytosis) and chlorpromazine (an inhibitor of clathrin-mediated endocytosis) did not exhibit any blockade, suggesting that the pathway is unconventional, possibly involving cell-surface engineering and the phagocytosis pathway.

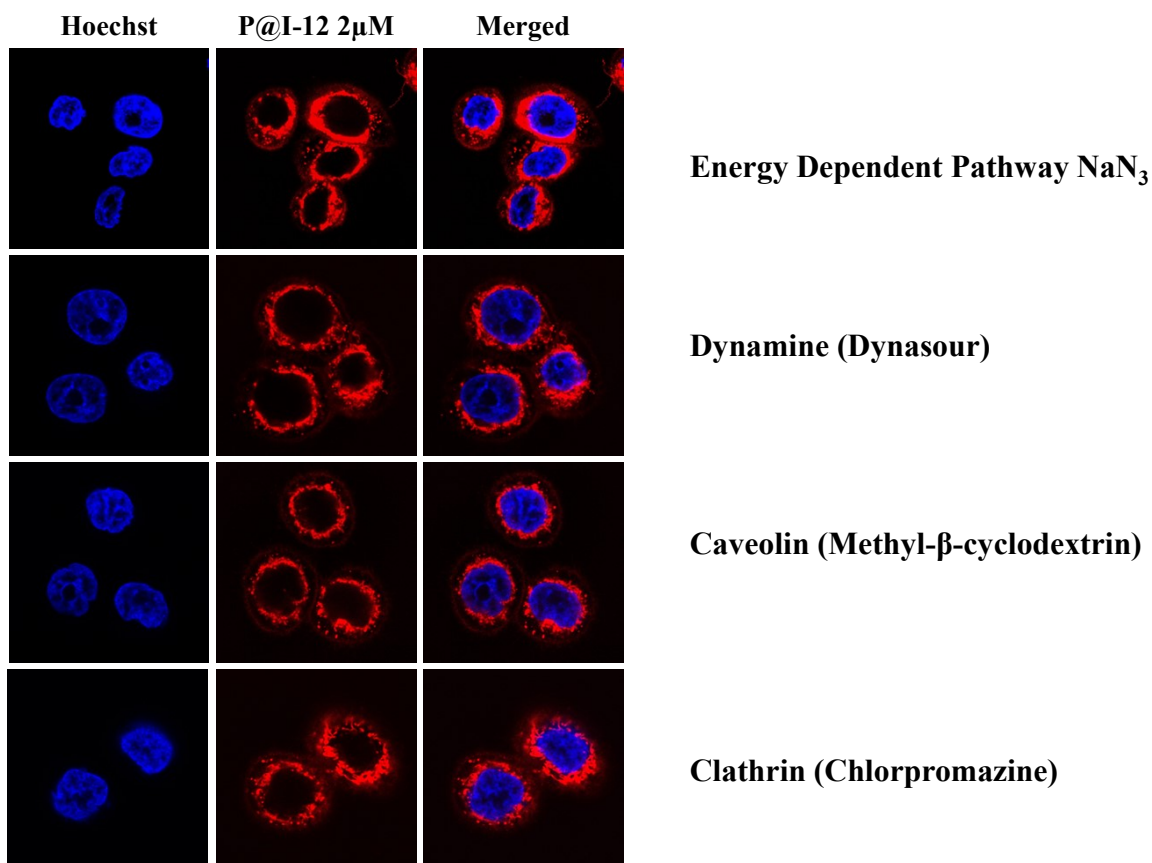


Figure S20. Confocal microscopy images of P-I12 in presence of different endocytotic pathway inhibitors.

10. MTT assay:

MTT assay was used to check cell proliferation. Cells (5×10^3 cells per well) were plated in 96 well plate in DMEM medium and incubated overnight followed by treatment with

different concentration of **P-I12** and fix concentration of cisplatin (Concentration nearby IC_{50} concentration) and further incubation for 48 h. Afterward 10 μ l of MTT (5 mg/ml) reagent was added to each well and incubated plates further for 4h at 37 °C. Purple precipitate formed was dissolved by adding 100 μ l of DMSO and plate was read at 570 nm.

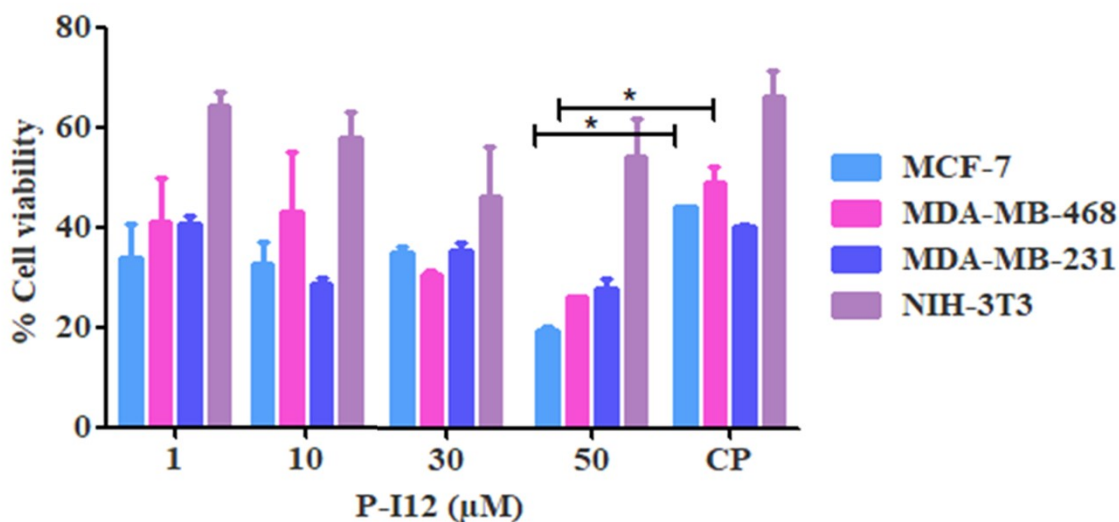


Figure S21. Cell viability for different cancer cells and normal cell in presence of cisplatin alone (CP concentration for NIH-3T3 25 μ M, for rest of cells 15 μ M) and in presence of mixture of **P-I12** and Cisplatin

To comprehend the cisplatin delivery mediated by P-I12, a cell viability assay was conducted on heparinase-treated MDA-MB-468 cell lines. Initially, cancer cells were cultured on a 96-well plate and treated with heparinase enzyme (100 ng/mL) (Sigma Aldrich, cat no. SAE0116) for 1 hour following the literature protocol.⁷ Subsequently, the cells were treated with different concentrations of peptides alongside cisplatin and peptides alone, all at an optimal concentration of CP (3 μ M), which induced 50% cell viability. Figure S18 illustrates that with an increasing concentration of the peptide, cisplatin-mediated toxicity also

escalated.

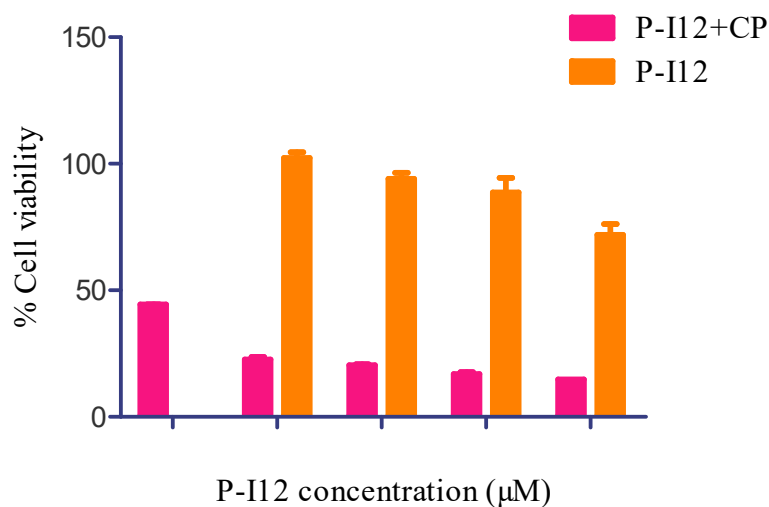


Figure S22. Cell viability assay with heparinase treated MDA-MB-468 cancer cells. Concentration of cisplatin alone was 3 μM .

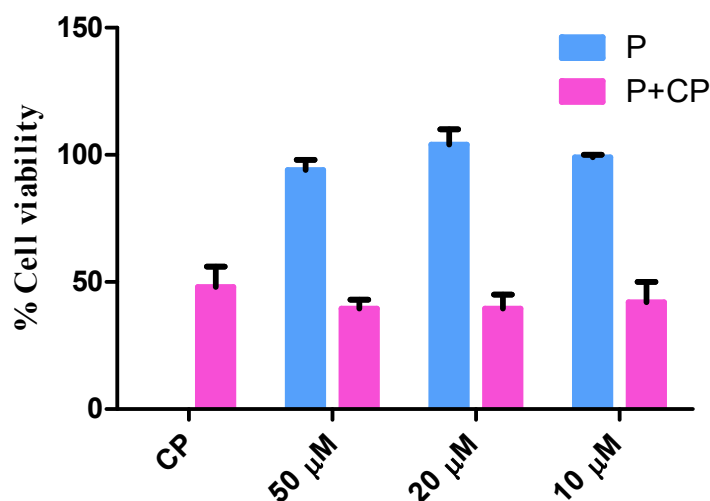


Figure S23: Cell viability assay with peptide without I12 ligand with MDA-MB-468 cancer cell at three different concentration in the presence of cisplatin 3 μM .

11. ICP-MS Analysis:

To further confirm cisplatin-mediated toxicity, ICP-MS was performed to measure the platinum concentration inside the cells. For this purpose, MDA-MB 468 cell first treated with heparinase enzyme followed by treatment with peptide alongside cisplatin and cisplatin alone for 48h. Cell pellets were collected digested with nitric acid, and subjected to ICP-MS. The observed concentration of CP inside the cells ranged between 2.5-2.8 μM with P-I12-treated

cells, while the concentration of CP in the absence of P-I12 was 1.5-2 μM . This indicates that the amount of the compound is doubled in the presence of P-I12.

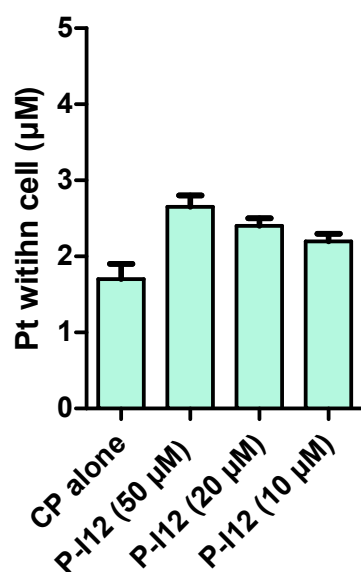
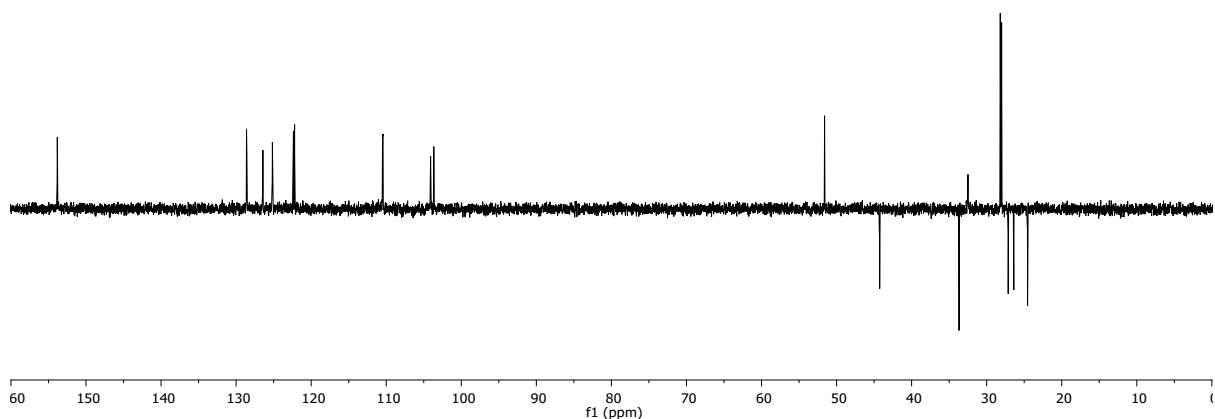
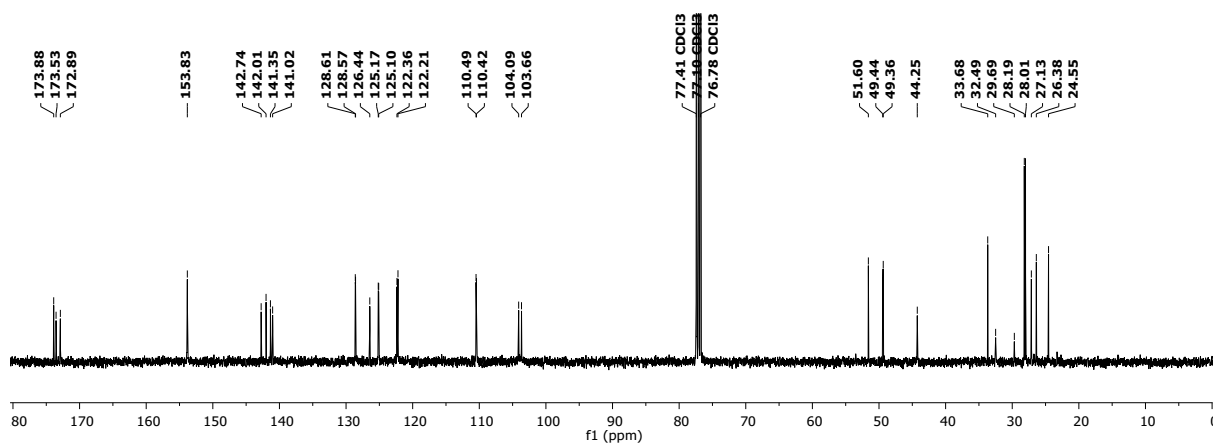
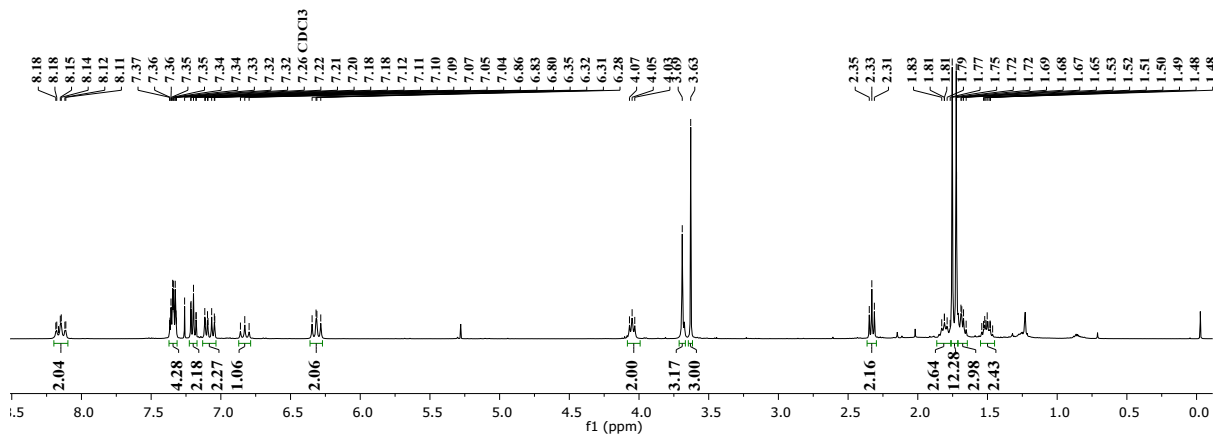
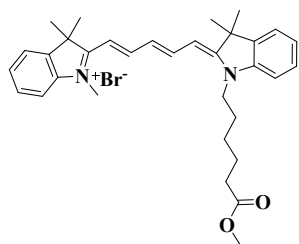


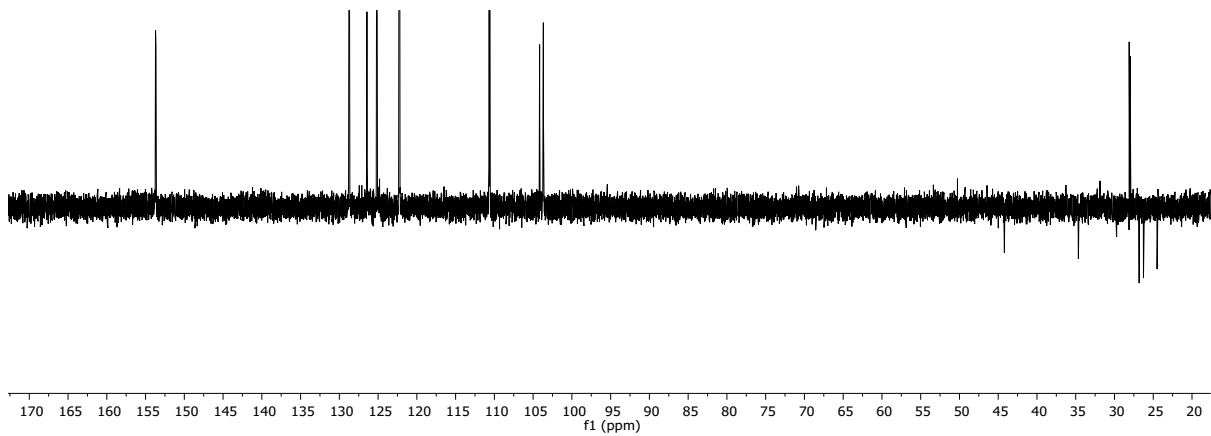
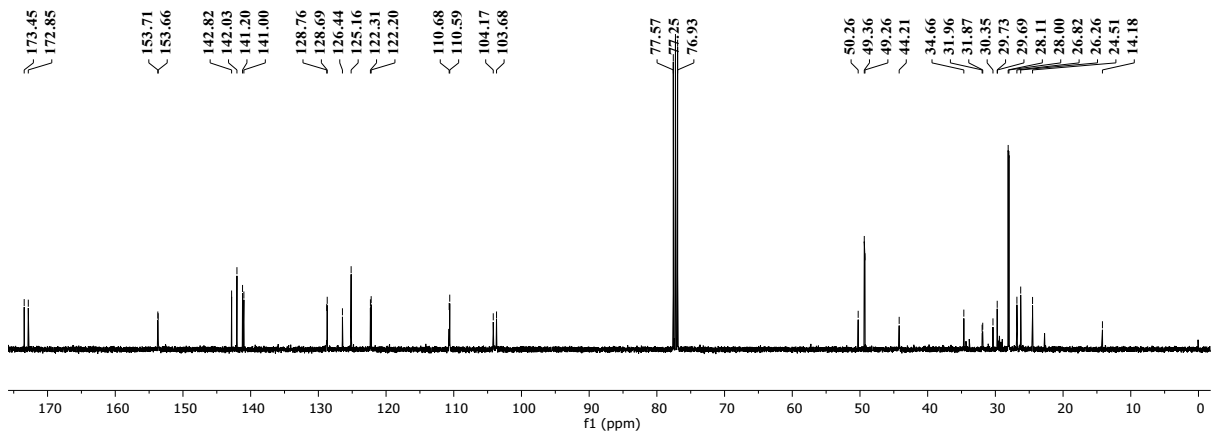
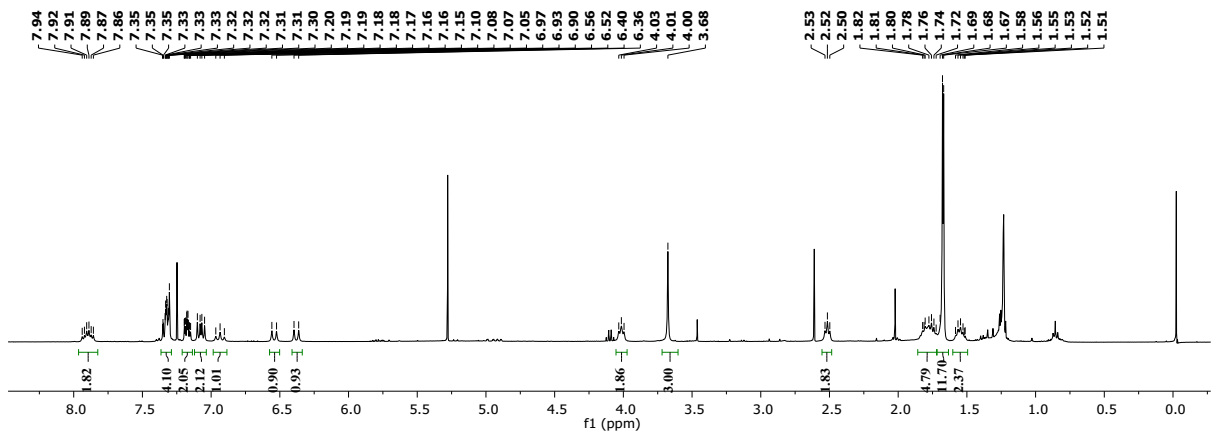
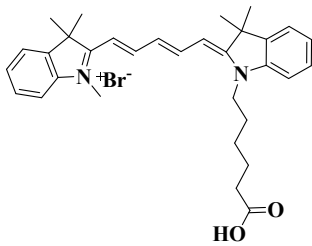
Figure S24. ICP-MS data for Platinum concentration within heparinase treated MDA-MB-468 cancer cells. Concentration of cisplatin alone was 3 μM .

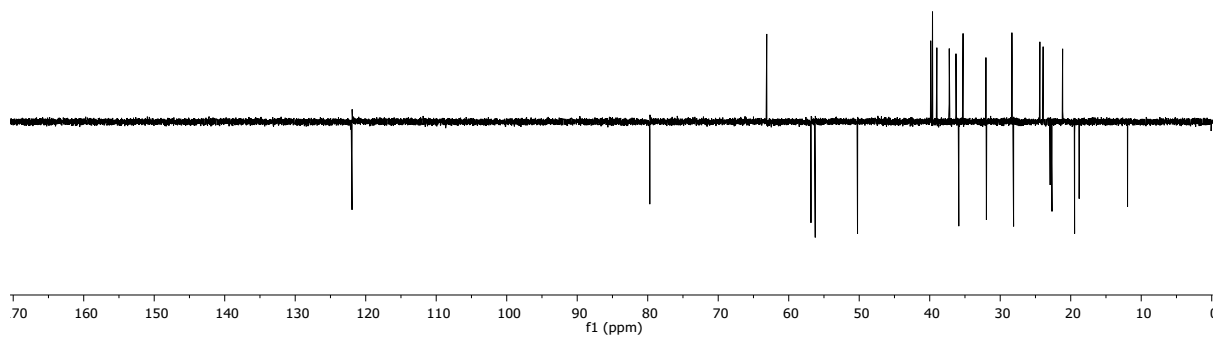
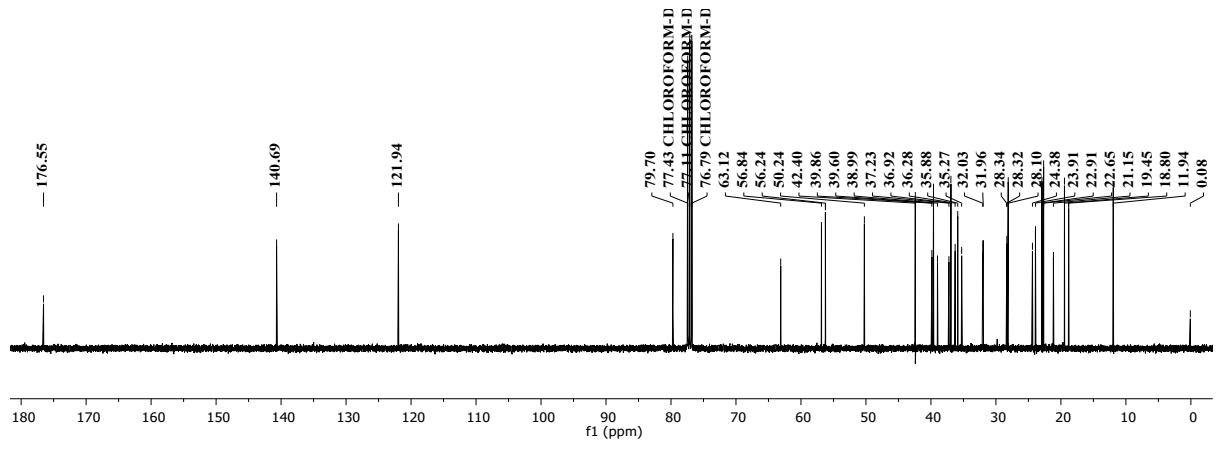
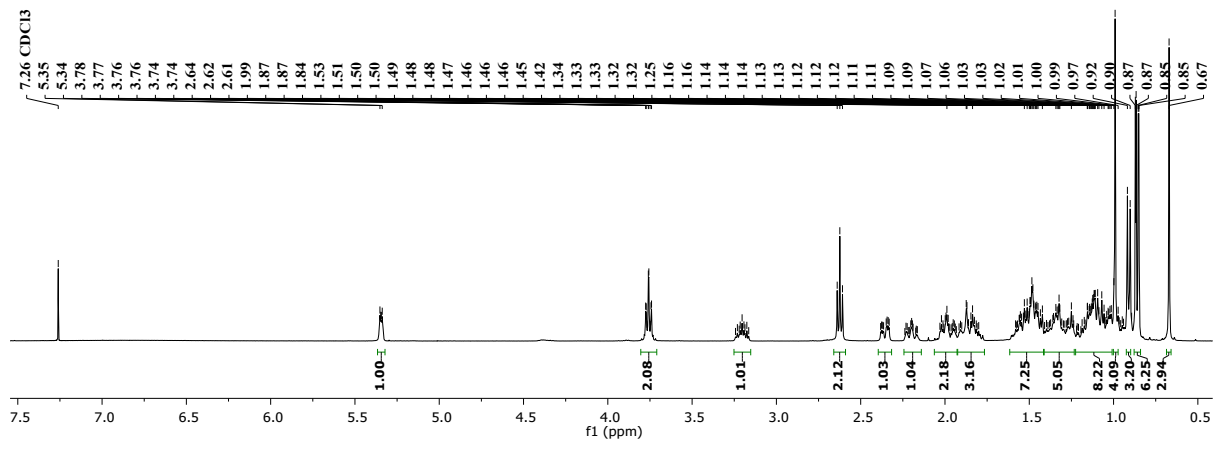
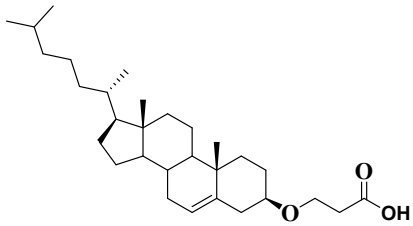
12. Reference.

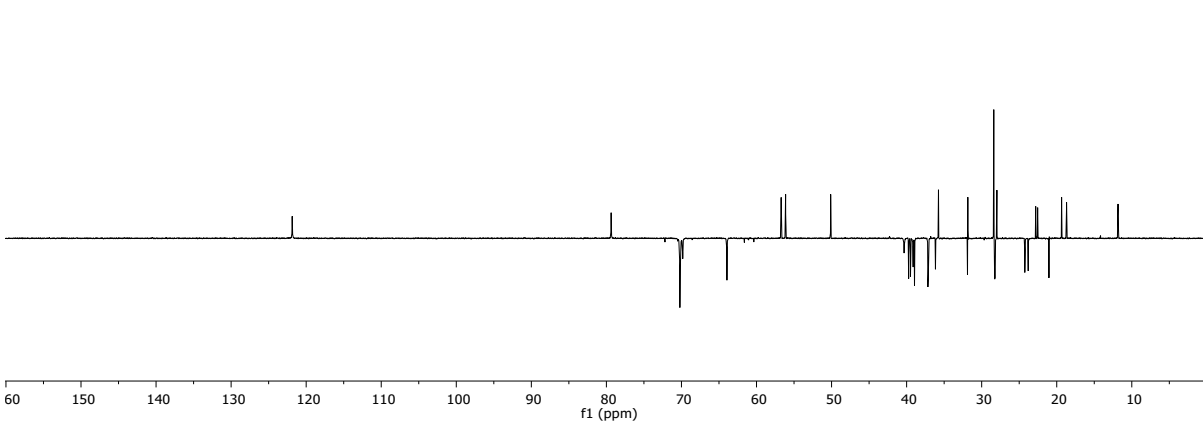
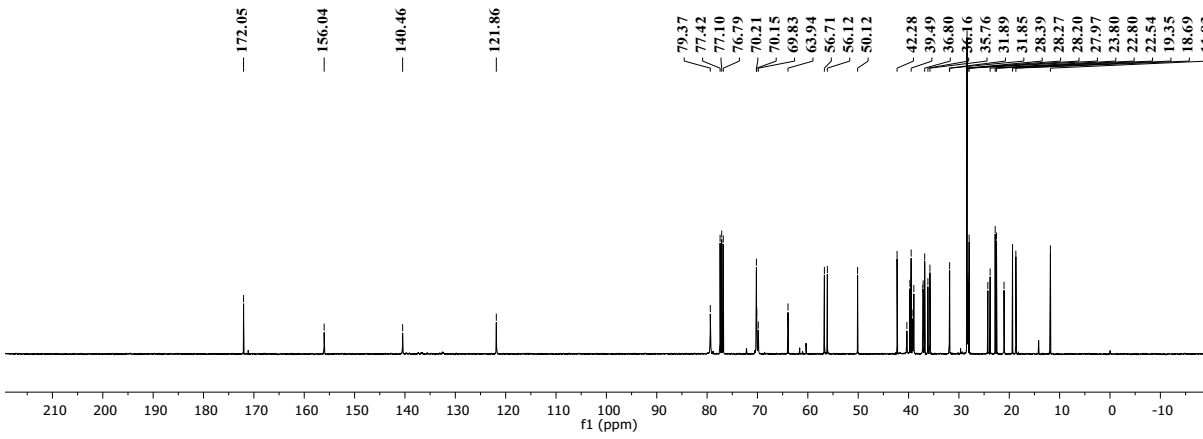
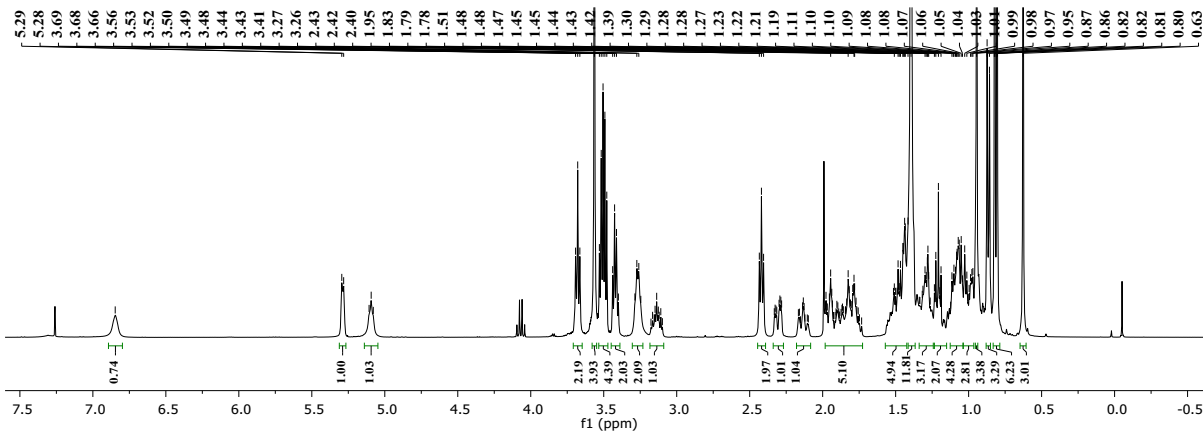
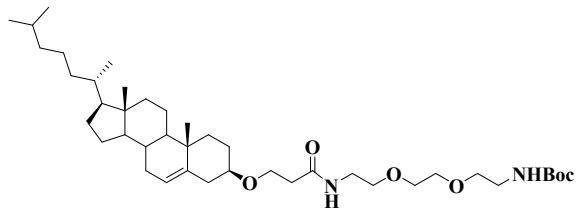
1. B. Subramani, C. D. Shantamurthy, P. Maru, M. A. Belekar, S. Mardhekar, D. Shanmugam, R. Kikkeri. *Org. Biomol. Chem.* **2019**, *17*, 4535-4542.
2. N. Bloembergen, E. M. Purcell, R. V. Pound, R.V., *Physical Review*, **1948**, *73*, 679-746.
3. E. O. Stejskal, J. E. Tanner, *J. Chem. Phys.* **1965**, *42*, 288-292
4. Pregosin, P. S.; Anil Kumar, P. G.; Fernández, I., *Chem. Rev.* **2005**, *105*, 2977-2998.
5. Anil Kumar, P. G.; Pregosin, P. S., *Organometallics*, **2004**, *23*, 5410-5418.
6. Chen, D. Wu, J. C. S. Johnson, *J. Am. Chem. Soc.* **1995**, *117*, 7965
7. Snigireva, A. V., Vrublevskaaya, V. V., Afanasyev, V. N. & Morenkov, O. S., *Cell Adhes. Migr.* **2015**, *9*, 460-468 .

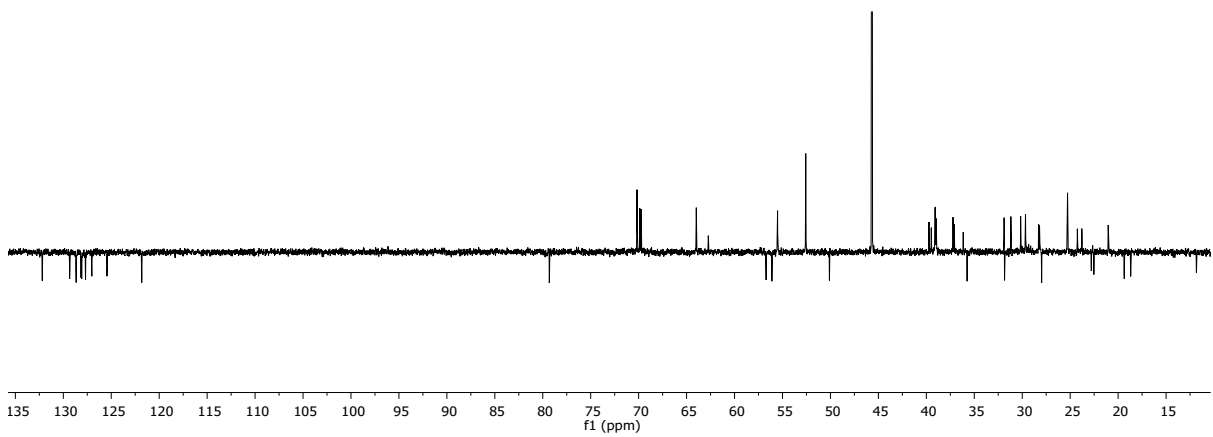
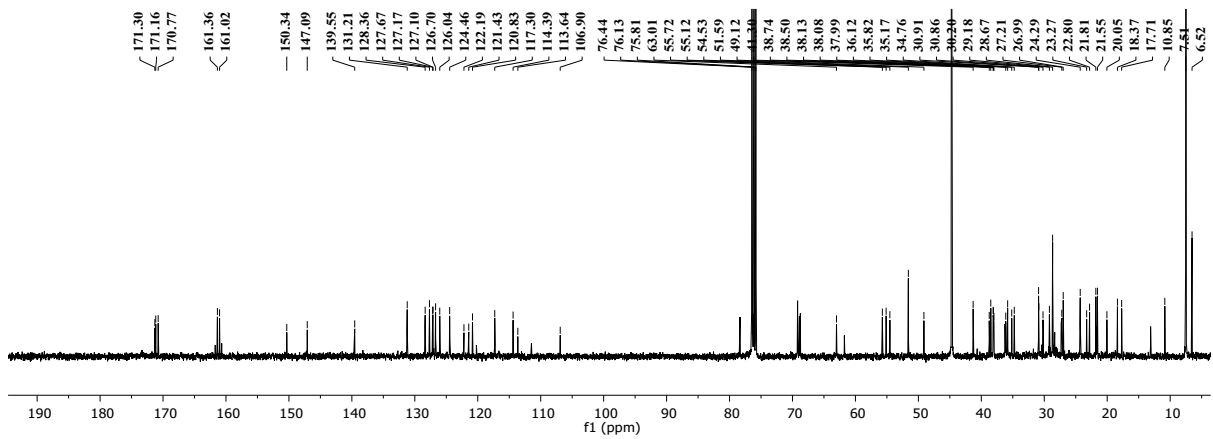
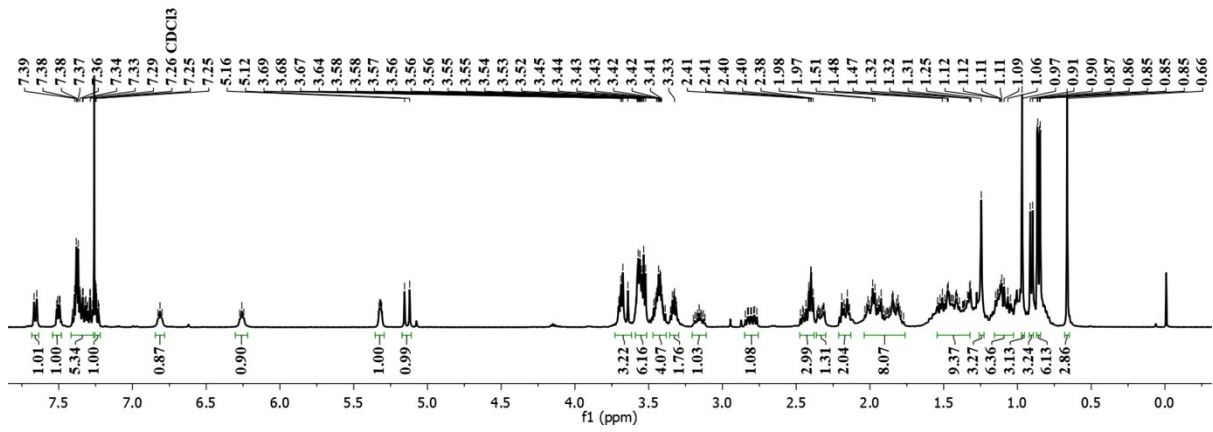
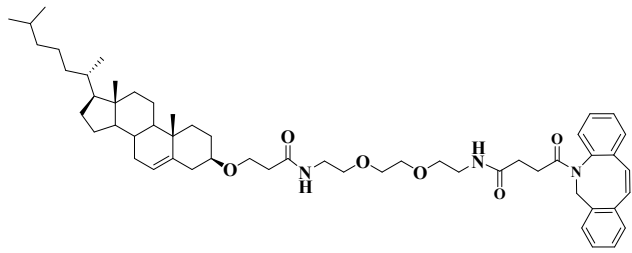
13. ¹H-NMR, ¹³C and DEPT-135 NMR



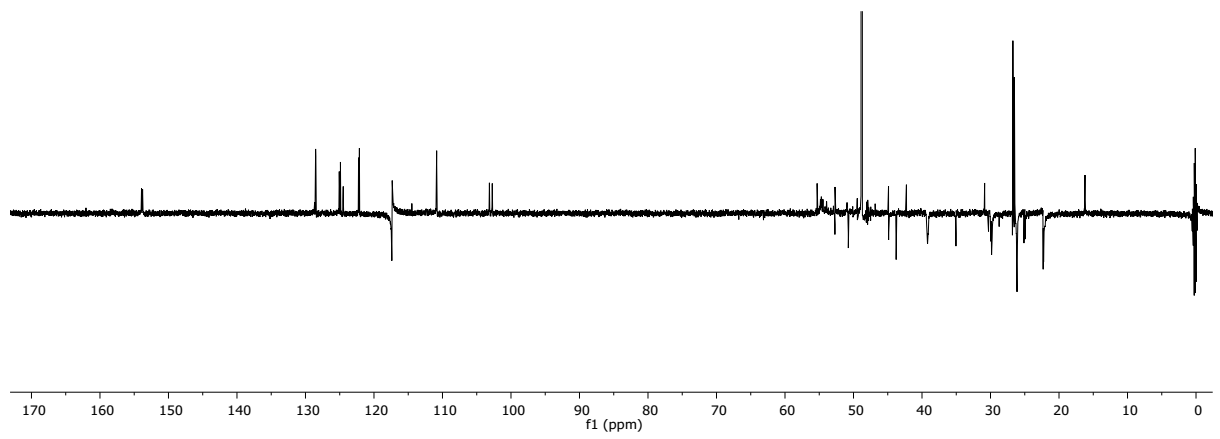
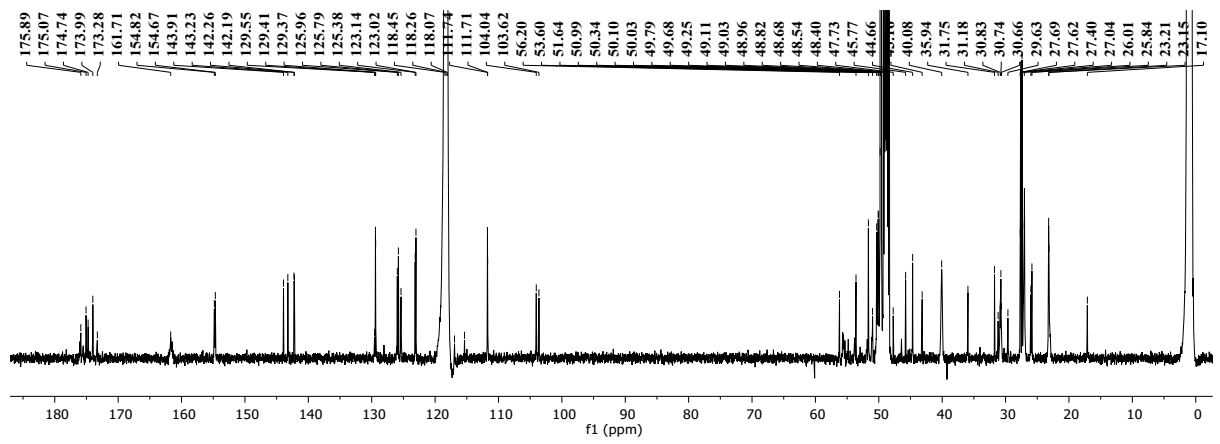
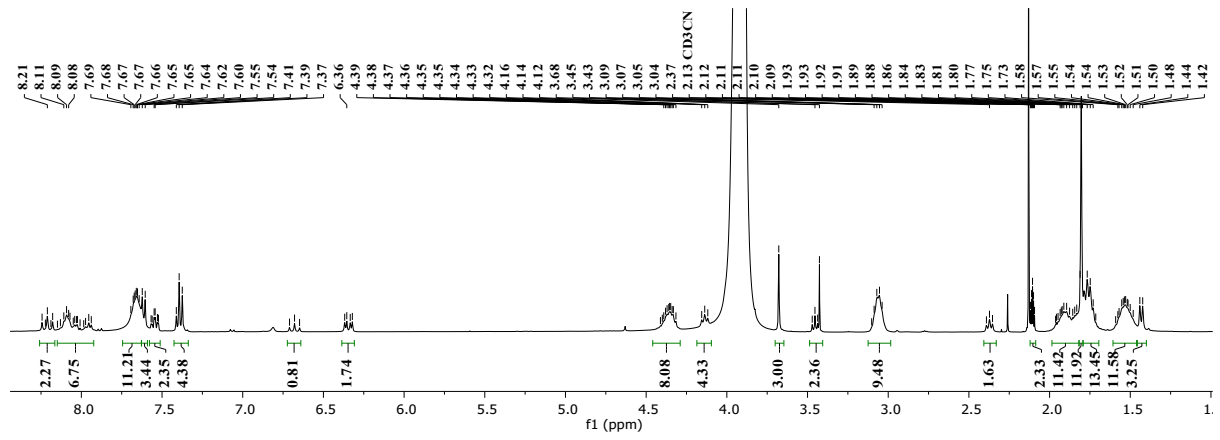
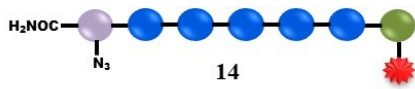


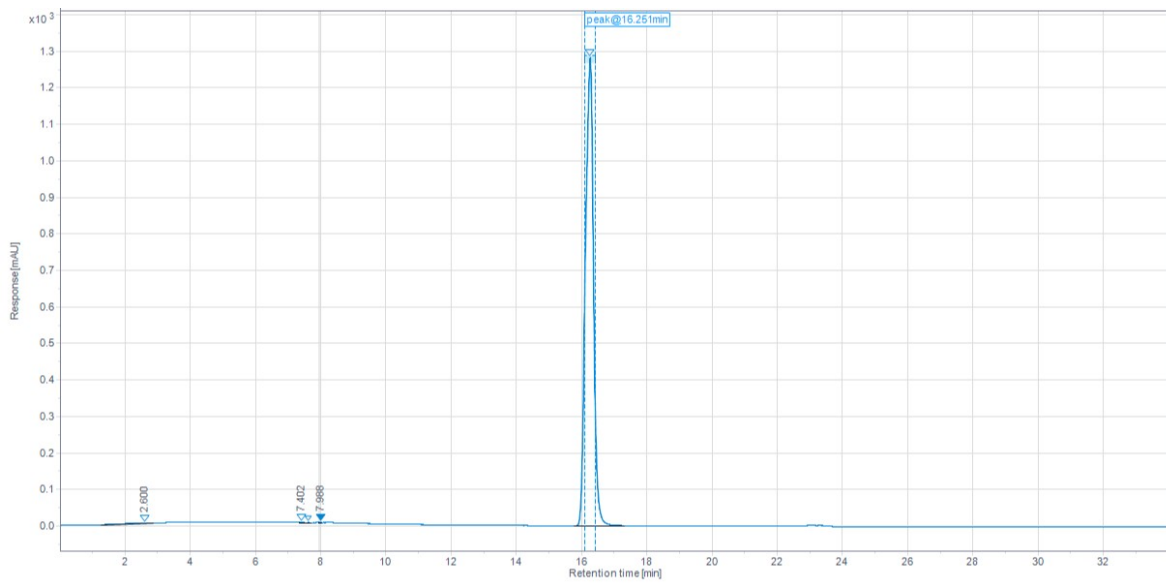
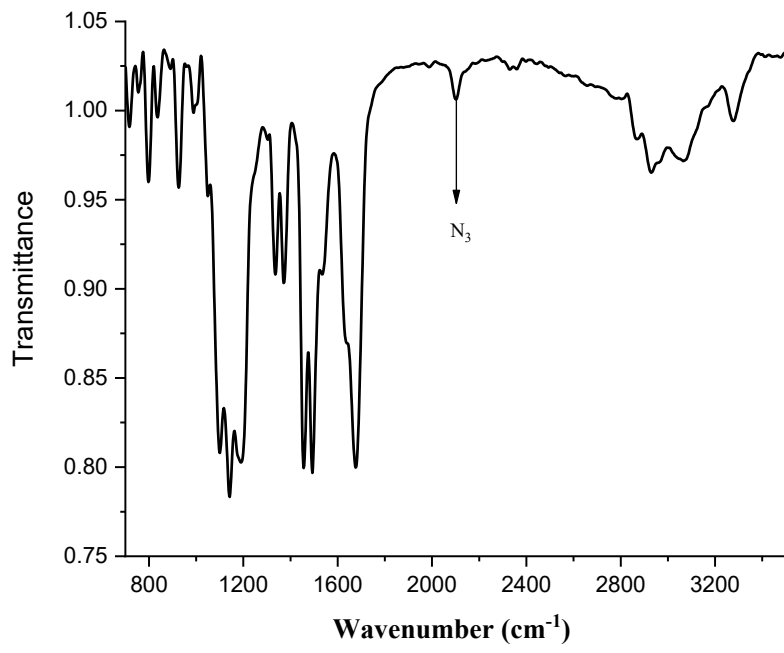




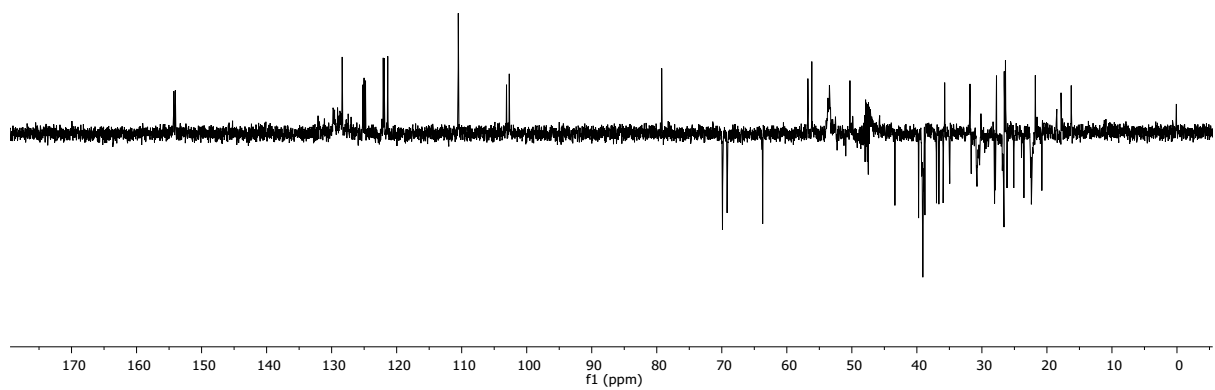
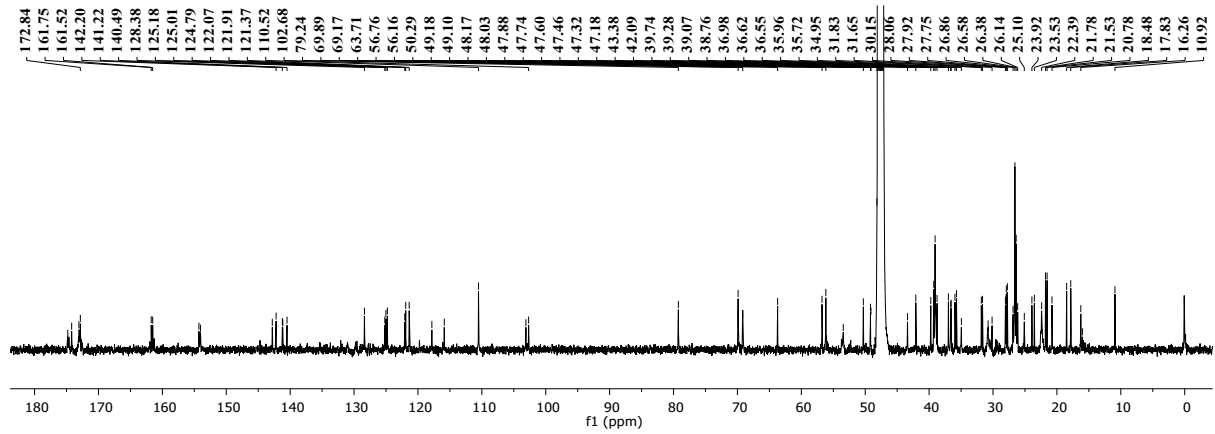
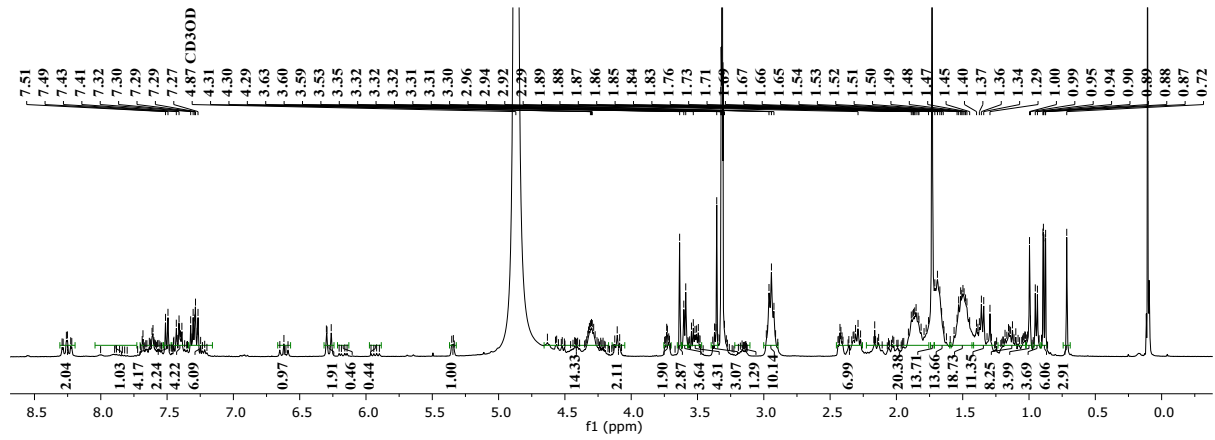
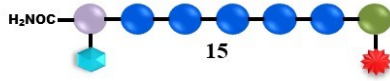


Compound 8:

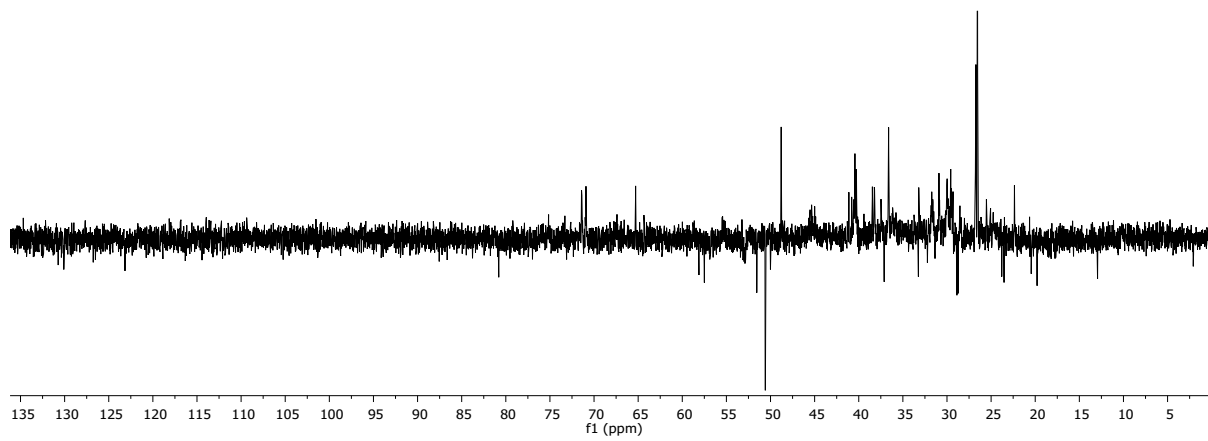
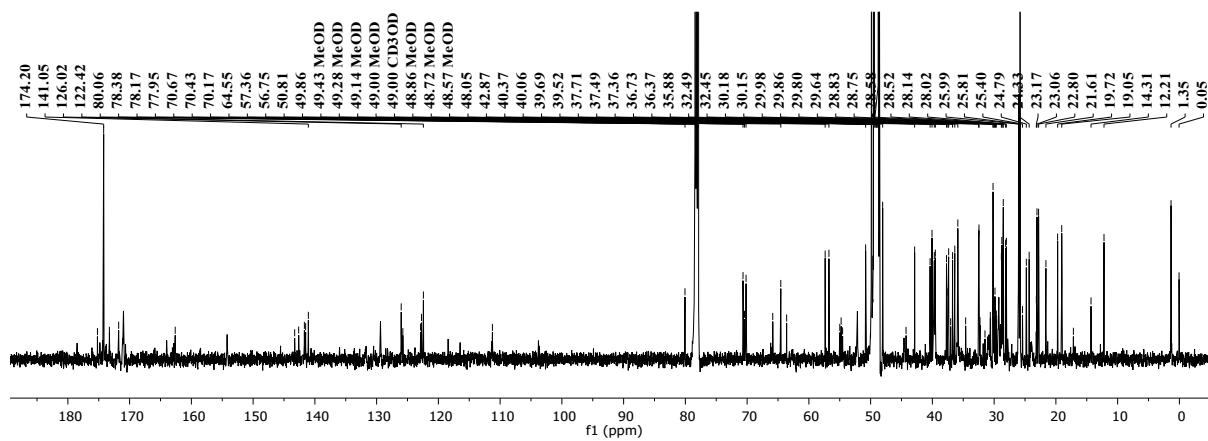
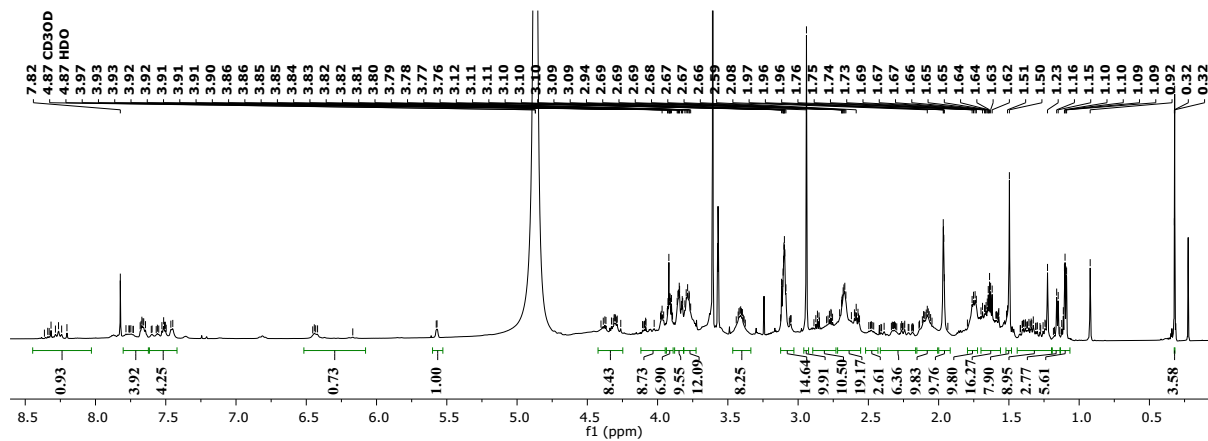
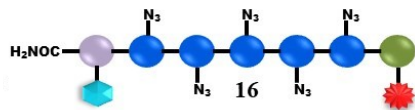


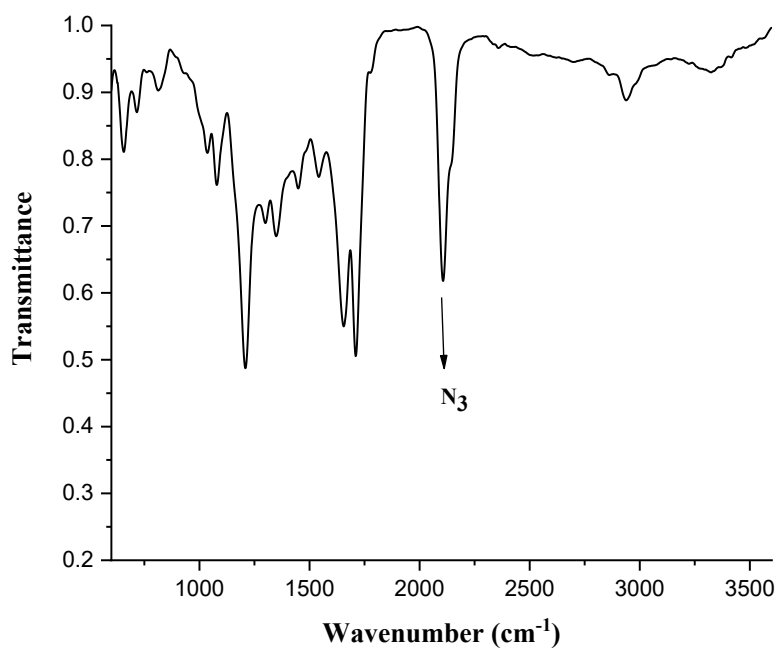


Compound 9:

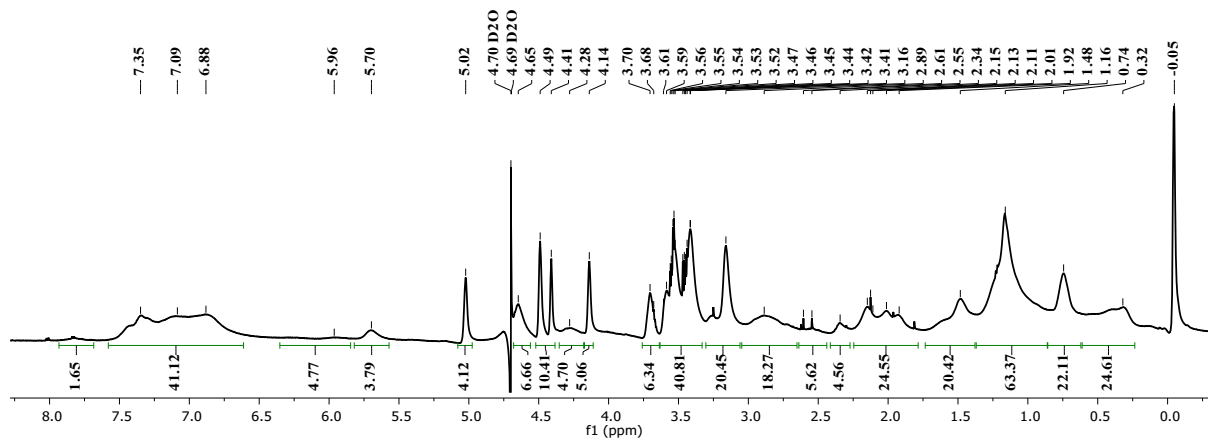
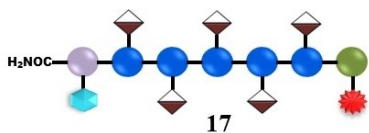


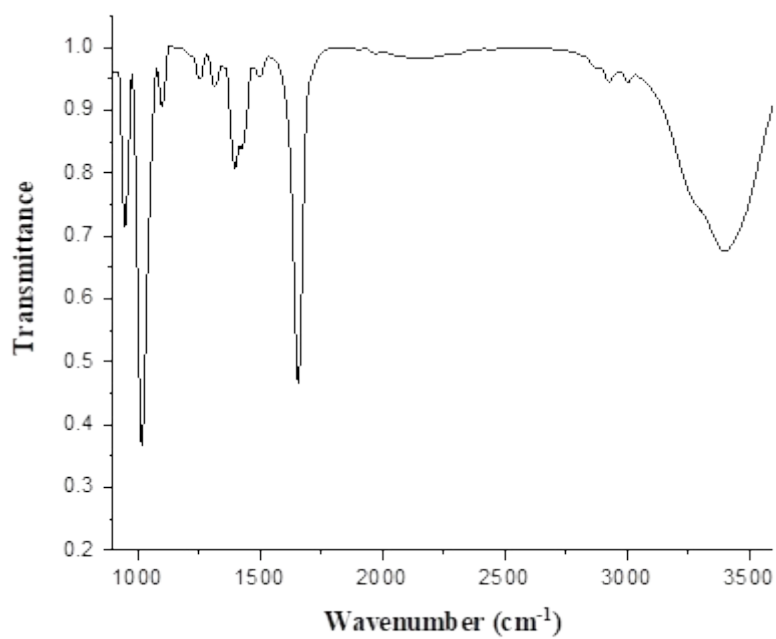
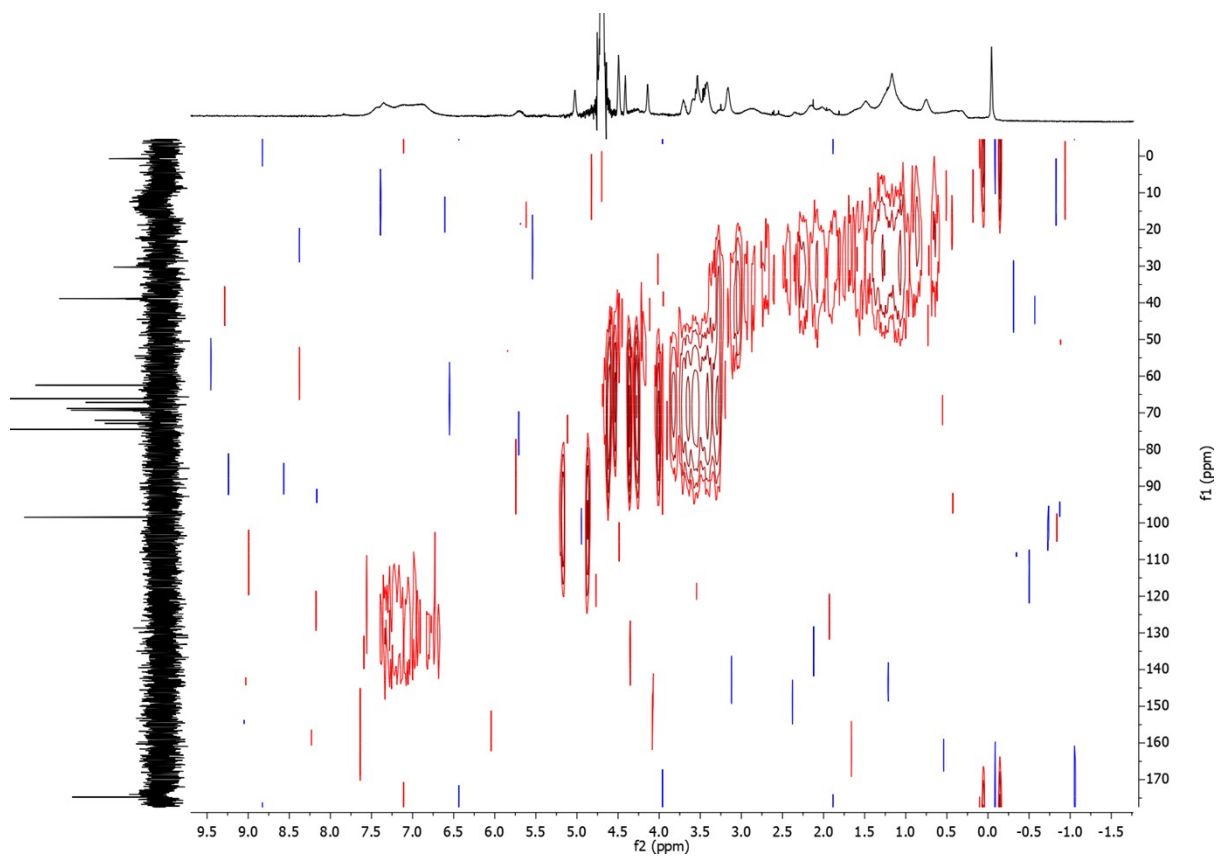
Compound 10:



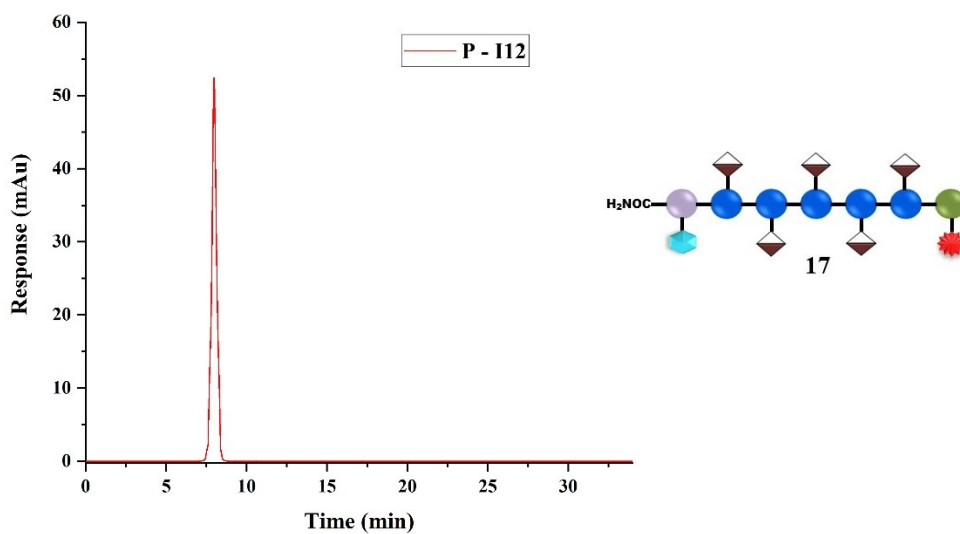


Compound 11:

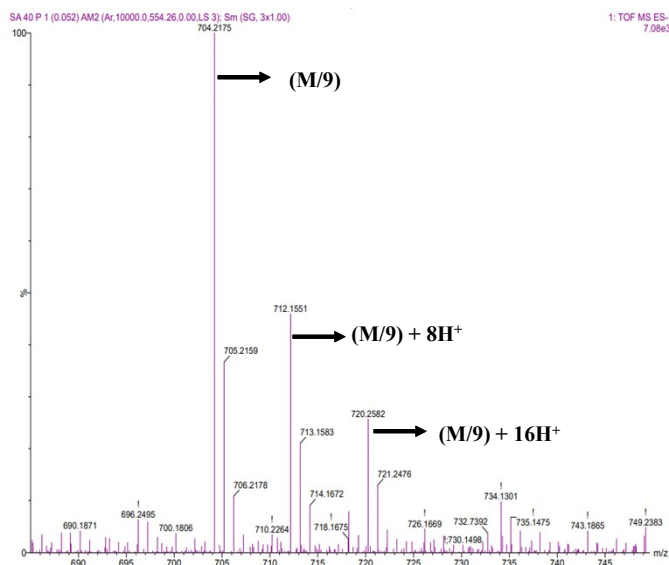




14. HPLC profile of compound 11 :-



HR-ESI-MS Data of compound 11 :-



UV absorbance for compound 11:

